

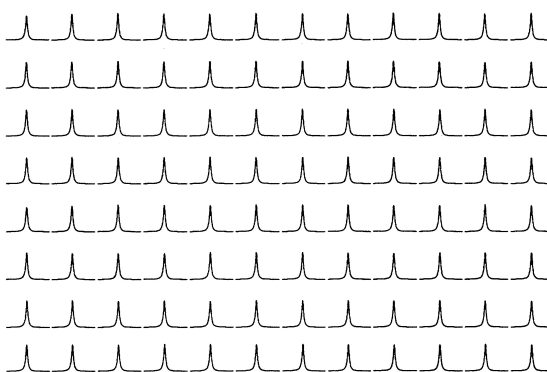
Direct-Injection NMR (DI-NMR): A Flow NMR Technique for the Analysis of Combinatorial Chemistry Libraries

Paul A. Keifer, Stephen H. Smallcombe, Evan H. Williams, Karen E. Salomon, Gabriel Mendez, John L. Belletire, and Cathy D. Moore

J. Comb. Chem., **2000**, 2 (2), 151-171 • DOI: 10.1021/cc990066u • Publication Date (Web): 19 February 2000

Downloaded from <http://pubs.acs.org> on March 20, 2009

DI-NMR



More About This Article

Additional resources and features associated with this article are available within the HTML version:

- Supporting Information
- Links to the 1 articles that cite this article, as of the time of this article download
- Access to high resolution figures
- Links to articles and content related to this article
- Copyright permission to reproduce figures and/or text from this article

[View the Full Text HTML](#)



Direct-Injection NMR (DI-NMR): A Flow NMR Technique for the Analysis of Combinatorial Chemistry Libraries¹

Paul A. Keifer,^{*,†} Stephen H. Smallcombe,[†] Evan H. Williams,[†] Karen E. Salomon,[†]
Gabriel Mendez,[‡] John L. Belletire,[‡] and Cathy D. Moore[‡]

*Varian NMR Systems, 3120 Hansen Way D-298, Palo Alto, California 94304-1030, and
Alanex Division of Agouron Pharmaceuticals, Inc., A Warner-Lambert Company,
3550 General Atomics Court, San Diego, California 92121-1194*

Received October 25, 1999

A new tool for analyzing compound libraries by NMR has been developed. Aliquots of solution-state samples (between 120 and 350 μ L) are directly injected, using a standard liquids handler, into an NMR (LC-NMR) flow probe. Automated NMR software tracks—and suppresses—intense signals arising from the nondeuterated solvents used (if any) and acquires high-sensitivity one-dimensional ¹H NMR spectra. An 88-member combinatorial library, dissolved in DMSO and stored in a 96-well microtiter plate, has been analyzed a number of ways using this technique. This nondestructive technique, which we call direct-injection NMR (DI-NMR) and which is embodied in our versatile automated sample changer (VAST) hardware, has proven to be both routine and robust. Our success in automatically acquiring the NMR data for entire plates of library compounds (within 4–8 h) has caused us to develop new ways to display and analyze the resulting NMR data, as will be shown here.

Introduction

Combinatorial chemistry has clearly evolved into a useful tool for many kinds of studies, especially those involving drug discovery and optimization.^{2,3} It has long been recognized, however, that one of the weaker aspects of combinatorial chemistry is the difficulty of obtaining a complete sample analysis.^{4–6} This paper introduces a new and novel method for the rapid and sensitive acquisition of ¹H NMR spectra on solution-phase combinatorial-chemistry libraries. The technique is based upon a direct-injection modification of stopped-flow LC-NMR spectroscopy.

Because NMR spectroscopy is typically considered to be one of the more powerful and information-rich analytical techniques, we have been investigating ways to enhance the role of NMR in combinatorial chemistry. We first pioneered the techniques for acquiring high-resolution ¹H NMR spectra of compounds bound to solid-phase-synthesis resins.^{7–11} Although these techniques are effective and are now widely used,^{12,13} we also recognized that they might not be suitable for the analysis of large libraries due to the difficulties of automating the sample preparation.¹⁴ At the same time, however, we were developing several new techniques in the otherwise unrelated area of HPLC-NMR.^{15,16} We recognized that some of these LC-NMR techniques could be used to develop an automated sample changer based upon flow NMR.^{12–14,17} We are reporting here that the increased automation and throughput of the resulting flow-NMR sample changer is lending itself nicely to the analysis of combinatorial-chemistry libraries.

Background

Combinatorial chemistry has several characteristics that have contributed not only to its success but which also present challenges to the analytical techniques that have traditionally been used for compound characterization. First, combinatorial chemistry typically produces larger numbers of compounds than does conventional synthetic chemistry, so any proposed analytical method should have an increased throughput capacity. Second, it typically produces smaller quantities of each compound, so the analytical method should exhibit an increased sensitivity. Last, it has de-emphasized the use of traditional glassware (such as round-bottom glass flasks) for synthesis and has emphasized the use of 96-well microtiter plates to both store and transport (and sometimes even to synthesize) the compounds of interest. This suggests that the analytical method should be able to handle samples stored in microtiter plates (as well as a wide range of other standard sample containers). The flow-NMR sample changer described here was designed to address all three of these issues. It reduces the cost, time, and effort of sample handling, it allows inexpensive sample containers to be used, and it uses smaller quantities of sample than traditional automated NMR systems.

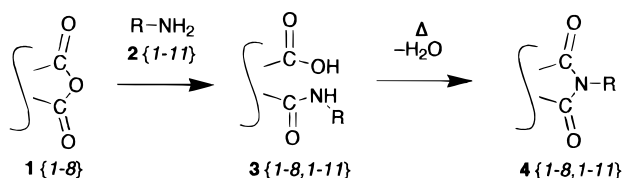
Combinatorial chemistry has also given chemists the flexibility to produce any given library as either a mixture of compounds or as a collection of pure compounds and to produce each of these either bound to solid-phase-synthesis resins or in solution. Unfortunately, however, no one known NMR technique has the flexibility to properly, rapidly, and easily analyze all four resulting combinations of these sample types. All combinatorial-chemistry samples are grouped by NMR into one of two general categories—solution-state

* To whom correspondence should be addressed. Phone: 650-424-5237.
Fax: 650-852-9688. E-mail: paul.keifer@varianinc.com.

[†] Varian.

[‡] Agouron.

Scheme 1



samples that are physically homogeneous (filterable) versus everything else—because different NMR hardware (e.g., a different probe) is required in each case to optimize the NMR analysis (for reasons which have been explained elsewhere⁸).

Solution-state samples (or more specifically, those samples which have a uniform magnetic susceptibility) can be analyzed in any style of cylindrical tube which is aligned with the Z axis of the magnet. This includes not only the conventional 5 mm precision glass sample tubes that are routinely used in NMR, but also samples contained in the flow-through detection cells found in the “flow probes” routinely being used for LC-NMR and related techniques. The growing popularity of these techniques is causing flow-style probes to become widely accepted. In flow probes (which usually have a fixed sample volume) the NMR sensitivities are relatively high due to their increased filling factors. (Because the fixed flow cell does not allow sample spinning, the rf coil can be mounted closer to the sample. This results in a slightly increased “filling factor” for the coil, which produces an increased NMR sensitivity.) The direct-injection NMR (DI-NMR) technique presented here is based upon our use of this style of flow probe.

The analysis of samples which are not physically homogeneous, such as compounds bound to solid-phase-synthesis resins, normally requires the use of other NMR techniques, such as magic-angle spinning (MAS). These techniques are discussed elsewhere.^{7–14} The flow NMR technique presented here is not appropriate for analyzing these kinds of samples.

Experimental Section

The 88-member (one-compound-per-well) test plate used in this investigation was synthesized entirely using solution-state methods. Because it was a test plate, and test plates are run to understand the scope and limitations of the chemistry, not all reactions in the plate yielded the intended product. In the plate, eight different cyclic anhydrides **1**{1–8} were dissolved in an aprotic polar solvent and reacted with eleven different primary amines **2**{1–11}, in a combinatorial fashion, to afford the intermediate amide-acids **3**{1–8, 1–11} (Scheme 1). Cyclic dehydration at elevated temperatures, along with removal of the solvent under vacuum, afforded the 88 different crude imides **4**{1–8, 1–11}. The resulting compounds were reconstituted with either DMSO-*h*₆ or DMSO-*d*₆, dispensed into 96-well microtiter plates, diluted to a known sample concentration (either 25 or 2.5 mM), and analyzed without further purification. Three kinds of daughter plates were made using this 88-member library: a 25 mM plate in DMSO-*h*₆, a 2.5 mM plate in DMSO-*h*₆, and a 2.5 mM plate in DMSO-*d*₆. The daughter plates contained 0.9 mL aliquots of each solution in separate wells of 1 mL volume (deep-well) polypropylene microtiter plates. Two plates which had been

made up during a preliminary phase of this investigation were found to contain unintended solvent impurities that complicated the data interpretation (see the Discussion section); these plates were re-dried under vacuum and reconstituted with a higher-purity grade of DMSO-*h*₆.

The NMR spectra were acquired on a standard UNITY-INOVA 500 MHz spectrometer which was equipped with a standard VAST liquids-handler accessory, a standard Z-axis-PFG triple-resonance (H{C,N}) flow probe (maintained at 20 °C), and VNMR 6.1B software. The flow probe had an active volume of 60 μL and a total flow-cell volume (minimum sample volume) of 115 μL. To fill the system (including the transfer tubing connecting the injector port to the probe), a total of 350 μL of sample was injected into the probe. (Much smaller sample volumes can be analyzed if push solvents are used.) After NMR analysis, the entire sample was withdrawn from the probe in standard fashion (described below) and returned to its original well. The spectra of the samples dissolved in DMSO-*h*₆ were run with single-frequency WET solvent suppression¹⁵ (using a 63 ms adjustable [dz] delay), SCOUT-scan automation,¹⁵ and ¹H gradient shimming; because there was no deuterated solvent there was no ²H lock. In contrast, the spectra of the samples dissolved in DMSO-*d*₆ were run without the use of solvent suppression and used both a ²H lock and ²H gradient shimming.¹⁸ The NMR probe was automatically washed with DMSO-*h*₆ after each sample injection, except for the samples dissolved in DMSO-*d*₆ which used DMSO-*d*₆ as a wash (rinse) solvent. Thirty-two scans plus two dummy scans, DSP oversampling,¹⁹ and a repetition rate of 1.95 s were used for each spectrum; this gives an NMR measurement time of 1 min for each sample. Total recycle time for each sample, including sample injection, shimming, acquisition, sample recovery, probe rinsing (one cycle), and automated plotting was 5.5 min per sample. Exponential line broadening (0.5 Hz), zero filling, and a single-frequency notch filter were applied to all spectra.

Discussion: Data Acquisition

In designing an NMR spectrometer to analyze combinatorial-chemistry libraries, the first concept we addressed was the fact that the system must be capable of analyzing thousands of samples without failure. Conventional automated NMR sample changers (i.e., those based upon 5 mm sample tubes) can have failure rates of several percent, and so they are not considered to be reliable enough for this task. Conventional sample changers can “fail” in a number of ways: the robot might mechanically break the tube, the automatic spinning of the sample can fail, the system may not be able to automatically find the ²H lock, the automatic shimming may fail, the automated receiver gain adjustment may fail, or the automated processing may not properly adjust either the vertical scale or the phasing of the spectrum. We recognized that a sample changer designed around a flow probe, using simple modifications of our LC-NMR techniques, could, with a few modest simplifications (vide infra), make many of these limitations disappear.

We also recognized that combinatorial chemistry was standardizing on a microtiter-plate format, so initially we

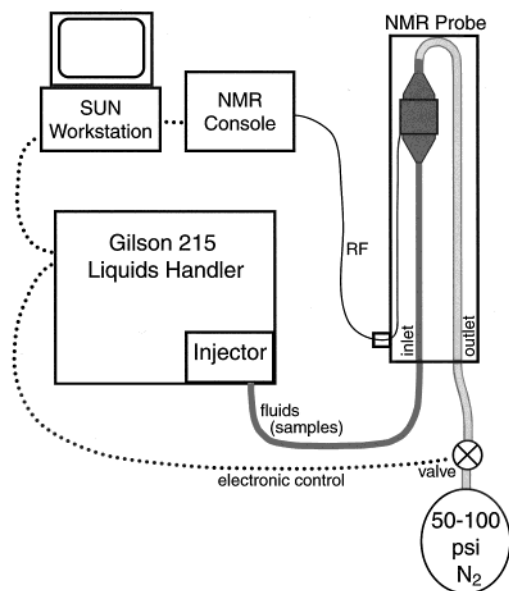


Figure 1. A block diagram of the VAST (versatile automated sample transport) DI-NMR (direct-injection NMR) system.

focused on the desire to acquire NMR data on samples stored in 96-well microtiter plates. The primary goal was to eliminate the need to transfer the samples into the precision glass tubes that are typically used for high-resolution NMR spectroscopy. Much of the cost of traditional NMR spectroscopy is incurred not only by the cost of the materials used (glass tubes and deuterated solvents) but also in the costs of drying the samples down (removing any protonated solvents so that the samples can be reconstituted in deuterated solvents), transferring the solutions to precision glass tubes, recovering the samples after analysis, and washing the glass tubes for re-use. Many of these problems could be addressed by using an automated liquid-handling device to take a sample solution stored in a microtiter plate and inject it directly into an NMR flow probe. This could be accomplished with any of several liquid-handler systems; we chose to use the Gilson Model 215 Liquids Handler²⁰ due to its wide acceptance within the combinatorial-chemistry community.

The complete sample-changer (VAST) system used for this study (as described below) is commercially available²¹ and was used without further modification. The hardware consisted of a Gilson 215 liquids handler, a Varian NMR flow probe, a switchable air valve (Valco), and the connective tubing (see Figure 1). The Gilson 215 was connected by an RS-232 control line to the spectrometer's host computer.²² All Gilson control codes were delivered by the software (VNMR) located on this workstation.²³ The standard Rheodyne injector valve located on the injector port was set to the inject position and never switched. The outlet of this injector valve was connected to the inlet port of the NMR flow probe (using a 65 in. \times 0.010 in. ID PEEK transfer line). Samples were stored in 96-well deep-well microtiter plates that were covered with 4 in. \times 5 in. sheets of Teflon-silicone-Teflon septum²⁴ and clamped into place inside Gilson 205H racks using the standard covers. Sample aliquots were aspirated from each well of the titer plate one-at-a-time and injected into the injector port. The volume of

injected sample solution (350 μ L) was calibrated to be sufficient to fill both the transfer line and the active region of the flow cell in the probe. The outlet port of the NMR probe was connected to a switchable Valco valve that was also connected to a source of high-pressure (55 psi) clean dry nitrogen.

The analysis of each sample was accomplished by the use of a fluidic "protocol" (a text file, written in Tcl/Tk, that defines each step of the analysis) and a series of parameters that controlled both the volumes and rates of all manipulations of the fluids. The standard "protocol" used in this study defined that the NMR flow cell started off empty, that the flow cell was to be rinsed once for each sample (prior to sample loading), and that each sample was to be recovered and returned to its original location after its NMR spectrum was acquired. When a start signal was generated by the NMR, the liquids handler aspirated a controlled volume of rinse solvent from a rinse reservoir and injected it into the probe at a controlled rate. When finished, the syringe reversed its direction of flow and withdrew this rinse solvent from the flow cell; when complete the liquids handler moved to the solvent-waste container and disposed of the rinse solvent. The liquids handler then moved to the appropriate sample container (here it was a well in a microtiter plate, but it could be a sample location in any one of a variety of possible sample containers). A controlled volume of the sample was aspirated from this container and then injected into the NMR probe via the injector port. When the sample injection was finished, a trigger was sent to the NMR to start the acquisition of all experiments listed in the experiment queue for that sample. (In this study, only a single 32-scan one-dimensional ¹H spectrum was acquired on each sample, but the software allows any number of additional experiments to be submitted into the experiment queue.) When the NMR acquisition was complete (and the experiment queue for that sample is empty), the NMR sent a signal back to the liquids handler, which used the syringe to withdraw the sample from the probe (pulling it back out the way it came in, as an intact column of liquid) and return the sample to its original container.

The operation of the syringe was synchronized with the Valco air valve. During injection, the Valco valve was open to the atmosphere, but during sample withdrawal, the Valco valve was switched to pressurize the outlet port of the probe. This back pressure allowed the speed of sample withdrawal to be increased. (The back pressure "pushes" the sample back while the syringe pump simultaneously "pulls" the sample back.)

A significant advantage of the current DI-NMR technique is that the maximum possible NMR sensitivity is obtained on each sample because the flow cell is empty when the sample is injected. A second advantage is that this also allows the sample to be recovered in an unaltered (undiluted) state. This is in contrast to the behavior observed when the flow cell starts off full of solvent (as is typical in LC-NMR), because in this case, the solvent left in the flow cell can dilute the incoming sample, which can both decrease the NMR sensitivity and alter (lower) the solution concentration of any recovered samples. The differences between these two

scenarios (injecting the sample into an empty flow cell versus into a flow cell full of solvent) illustrate how VAST, which is a specific implementation of DI-NMR, is very different from its possible alternative, flow-injection-analysis NMR (FIA-NMR).^{12,14,25} FIA-NMR, also known as “columnless LC-NMR” because there is no compound separation,^{12,14} is analogous to LC-NMR in that the sample and solvent flow in only one direction. This different fluid behavior of DI-NMR (as compared to FIA-NMR) influences many performance aspects of the analysis such as carryover, detection efficiency, recovery efficiency, and speed. As a consequence, DI-NMR has both advantages and disadvantages as compared to FIA-NMR.²⁵ The biggest disadvantage of DI-NMR (which is addressed by FIA-NMR) is the possibility that the tubing in the system could become clogged with particulate matter if unfiltered samples are injected.

We have also investigated the use of bubbles in DI-NMR to separate the sample and the solvent, and deemed this to be both unnecessary and undesirable in the current configuration. This is in accordance with other studies of the behavior of fluids in the presence of separating bubbles.^{26,27}

Although this automated DI-NMR sample changer (VAST) can be used in a wide range of applications, it is ideally suited to the analysis of combinatorial-chemistry libraries for three reasons. The first reason is that all members of a single combinatorial library are typically dissolved in the same solvent (or solvent mixture). This simplifies the NMR analysis in six ways: (A) It eliminates the need to worry about rinsing and drying the flow cell as completely as would be needed if immiscible solvents were allowed to be injected one after another. (B) It eliminates sudden changes in solvent composition that could cause sample precipitation and hence plug up the plumbing. (C) This also lessens the chance of creating physical heterogeneities of any sort—bubbles, suspensions, emulsions, or particles—caused by the previous sample or solvent, which, if present in the flow cell, could cause the NMR resonances to become broad and unshimmable. (D) It lessens the need for an operator to modify or optimize the acquisition or solvent-suppression parameters from sample to sample. (E) It lessens the shimming requirements from sample to sample (which saves time). (F) It lessens the need to tune the probe on each sample (which also saves time), and this also allows the spectral phasing to remain constant (which makes automated plotting more reliable).

The second reason for using DI-NMR is that most combinatorial libraries are composed of roughly equimolar-concentration solutions. This simplifies the analysis problem in four ways: (A) It reduces the problems caused by sample-to-sample carryover (if the carryover averages 1%, the NMR spectrum of any given sample would be significantly compromised if the previous sample was 100-fold more concentrated—this is much less of a problem if all the samples are the same concentration). (B) It lessens the need to optimize the receiver gain on each sample (the automated adjustment of the receiver gain not only takes time, but, as mentioned above, it is one of the possible failure modes of conventional NMR automation). (C) It lessens the need for an operator to interact with the parameter set for each sample,

which saves time and also facilitates quantitative comparisons, since each spectrum will be acquired under identical conditions (i.e., same number of transients). (D) It reduces the likelihood of autoscaling failures during processing (since each spectrum can be plotted with the same vertical scale). It will be shown later how useful it can be to have each spectrum from every well in a plate displayed in a directly comparable way. This can only happen if the receiver gain, the number of transients, and the plotted vertical scale are all held constant.

The third reason for using DI-NMR is that, in combinatorial chemistry, the structures of the compounds located in each well are usually known (or at least suspected), and the structures of the starting materials are known as well. This increases the likelihood of success in applying computer databases and/or spectral prediction software to simplify the problems of data interpretation.

The success of VAST has depended critically upon our use of a wide variety of otherwise unrelated NMR tools that, although initially developed for other NMR disciplines, have become important parts of the NMR toolkit for VAST. These tools include WET solvent suppression, the SCOUT-scan technique, DSP notch filters, ¹H and ²H gradient shimming, high-sensitivity NMR flow probes, and pre-existing software for the automation of conventional NMR spectroscopy.²³

The first core tool—WET solvent suppression¹⁵—is a technique that itself depends upon developments in shaped pulses, shifted laminar pulses,²⁸ pulsed-field gradients, and ¹³C decoupling.¹⁵ The advantages of WET are numerous. WET can suppress multiple NMR resonances at any number of frequencies and can do so with controllable (and different) bandwidths. It has a controllable shape of frequency selectivity (depending upon the shaped pulse used) and can selectively suppress the ¹³C satellites of organic solvent resonances without “bleaching” solute resonances located underneath these satellites. (This allows resonances hidden under these ¹³C satellites to be observed.¹⁵) It does place extreme demands upon the quality of the NMR hardware (both in the linearity and phase-shift timing of the rf as well as in the blanking behavior of the PFG amplifier), but if the spectrometer is up to it, WET suppression has proven to be very “robust” in the NMR sense. More so than any other equivalent solvent suppression technique, WET tolerates miset parameters (misset pulse widths, rf power levels, probe tuning, or small frequency offsets), and because it requires no parameter tweaking to make it work, it is easy to automate. Other solvent suppression schemes (like presat) have been evaluated and can be used if desired, but the advantages listed above may be lost. WET now allows us to routinely acquire ¹H NMR spectra on samples dissolved in either traditional deuterated solvents or in nondeuterated (protonated) solvents or solvent mixtures. (This should facilitate a user’s ability to use the same plates for both mass spectrometric and NMR analyses. A typical NMR solvent like D₂O can complicate the mass spectral data if variable amounts of ²H exchange occur within the sample.) Typical protonated solvents used to date have included CH₃CN, CH₃-OH, DMSO, H₂O, THF, CHCl₃, and mixtures thereof. Although WET is capable of suppressing multiple and/or

broad resonances (as would be observed for a solvent like ethanol), any solute signals at those frequencies will be lost; hence it is desirable to use solvents with singlet proton NMR resonances.

The second core tool is the SCOUT-scan technique.¹⁵ This tool allows us to automatically track the frequencies of the largest NMR resonances. The software allows a user to control at least four different parameters in the SCOUT-scan search algorithm, including how many frequencies should be suppressed and how wide their corresponding suppression bandwidths should be. The SCOUT-scan output information is then used to drive the WET suppression (described above), the DSP suppression (described below), and the resetting of the observe transmitter to an organic-solvent resonance (which affords us an active ¹H lock and a chemical-shift reference). The sequence of events in a SCOUT-scan are as follows: the current solvent-suppression parameters are temporarily stored, and the NMR parameters reset for a one-scan, small-tip angle (<1°), no-solvent-suppression experiment. A spectrum is acquired and then analyzed according to the SCOUT algorithm (in accordance with parameters entered by the user). The resulting information is used to both reset the transmitter to the appropriate reference line and to create the multiple-frequency selective pulse used for the WET suppression. Finally, the original solvent-suppression parameters are retrieved, updated, and the signal-averaged NMR spectrum is acquired. SCOUT-scan automation and WET suppression were used to acquire all the data in this paper shown on samples dissolved in DMSO-*h*₆.

Another solvent-suppression tool we can use is a frequency-selective notch filter—a low-pass form of digital signal processing (DSP). This data-processing technique is a standard, readily available tool which has proven itself useful in many fields of NMR.²⁹ Like WET, it can eliminate solvent resonances, but because it is a form of data processing and is applied only after the acquisition is complete, its effects are reversible (or can be “undone”). This is in stark contrast to acquisition-time solvent suppression—that which is controlled by the pulse-sequence—whose effects are a permanent part of the data. (The effects of WET suppression, for example, cannot be “undone” without re-acquiring the NMR data.) The effects of the notch filter are fully user-customizable. If the desired effect is not achieved the first time, the processing parameters can be altered and the data re-transformed using different values of the filter width, filter selectivity, and filter offset parameters (ssfilter, ssntaps, and sssfrq, respectively, in VNMR software). In addition, since the filter offset parameter (sslsfrq) can be arrayed, multiple resonances can be eliminated from the NMR spectrum quite easily. Because the DSP notch filters behave differently than the WET suppression, we find it particularly convenient to be able to choose either one at will and to have both techniques available for use either simultaneously (on the same resonance) or separately (on different resonances). We often default to applying the postacquisition DSP filter to all resonances that were suppressed with WET.

For reasons that are at least partly understood, we have found that the DSP filter frequency required to optimally remove a residual (suppressed) solvent signal may need to

be several hertz away from the frequency the same solvent resonance would have if it were unsuppressed.³⁰ The magnitude of this shift typically increases as the size of the unsuppressed signal gets larger.

While these tools now allow us to acquire data on samples dissolved in fully protonated solvents, this is not meant to suggest that the resulting spectra are fully identical to those acquired using deuterated solvents. A typical example is shown in Figure 2. Here, the bottom two spectra contrast the effect of acquiring data on the same sample dissolved to the same concentration in either DMSO-*h*₆ (using both WET suppression and a DSP notch filter) or DMSO-*d*₆ (using no solvent suppression or processing filter). The two spectra are essentially identical (neglecting differences in solvent impurities) except for the 0.4 ppm wide region around the solvent resonance at 2.5 ppm.

A final tool which we depend upon is high NMR sensitivity, which is influenced by both the probe and the NMR console. We were encouraged by our initial efforts in this project in which we were able to produce ¹H NMR data on samples as small as 5 μg.¹ (A solution containing 5 μg of solute within the 60 μL active region of the rf coil can produce spectra with a signal-to-noise of about 30:1 in about a minute.) Clearly, however, the minimum threshold of signal-to-noise that is acceptable in a spectrum depends upon whether one is trying to (1) determine the structure of a total unknown *de novo* (the typical goal in a natural products program); (2) verify the structure of a known compound and determine its purity level (the typical goal in combinatorial chemistry), or (3) merely detect the presence of a known compound. One of the goals of this paper is to document the typical performance of a VAST system and to verify that it can be used as an analytical tool for combinatorial-chemistry libraries.

Discussion: Data Analysis

After developing this method to acquire NMR data on every well in a microtiter plate (i.e., VAST), it rapidly became apparent that more sophisticated ways of dealing with the resulting mass of data were required. Previously, the default output from a conventional (non-VAST) NMR automation run was always just a stack of paper containing one spectrum per page. While this mode of plotting can still be used for titer plate samples, the resulting stacks of paper may start to overwhelm synthetic chemists as much as it helps them. We recognized that we could facilitate the analysis of DI-NMR data by using some of the data-processing tools that we had developed for LC-NMR.

The first tool is a process we call “gluing”, in which a collection of related one-dimensional ¹H spectra are added together to form one single larger file. The parameters of this larger file are modified to enable the collection to be treated (processed and plotted) as either an array of one-dimensional spectra or as a pseudo-2D data set. This allows us to use a wide variety of pre-existing tools developed for displaying and plotting both arrayed and 2D data sets. This gluing process also allows the data from an entire titer plate to be handled as one file; this facilitates bookkeeping, data archiving, and quantitative analyses (because identical

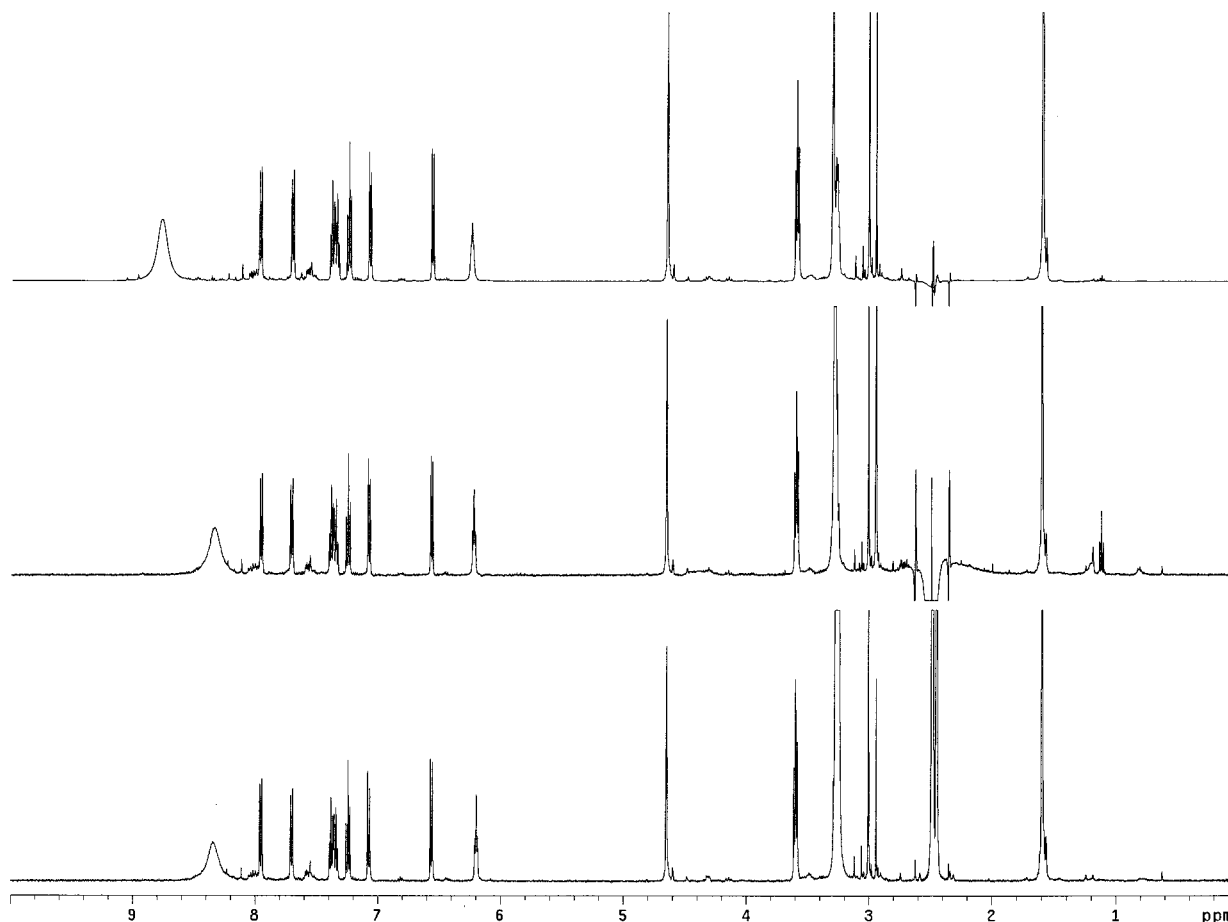


Figure 2. Proton NMR spectra acquired on a typical well (G8; 58) of the 25 mM DMSO- h_6 plate (top), the 2.5 mM DMSO- h_6 plate (middle), and the 2.5 mM DMSO- d_6 plate (bottom). The similar appearance of all three spectra shows that all three conditions (25 mM or 2.5 mM; DMSO- d_6 or DMSO- h_6) can be used to acquire VAST data within 1 min (32 scans). Note that the chemical shift for the broad anilide NH resonance is different in the 25 mM spectrum than in the 2.5 mM spectra (8.8 ppm versus 8.4 ppm). The DMSO- h_6 spectra (top and middle) were acquired with single-frequency WET solvent suppression (at 2.5 ppm) and a single-frequency DSP notch filter (ssfilter = 80). Neither solvent suppression nor notch-filter processing were used to acquire the DMSO- d_6 spectrum (bottom). The 25 mM spectrum was plotted with a 10 \times lower vertical scale to facilitate intensity comparisons with the 2.5 mM spectra. Otherwise, the same data acquisition, processing, and display parameters were used for all three spectra.

processing and plotting can easily be used for the entire collection of data). (Although the focus of this paper is to describe the use of glue in analyzing samples stored in microtiter plates, any number of spectra acquired on samples stored in any kind of sample container can be “glued” together.)

Once the data are glued, we can reshuffle, or display, or plot the data in a number of ways. Some of these data presentations work best as hardcopy (paper) plots, while other presentations are more effective as interactive displays on a computer monitor. Some presentations work well for long-term archiving of the data, while others are better suited for a detailed analysis of the data. Some presentations facilitate comparisons between the wells that are aligned along columns, while other displays emphasize comparisons along the (perpendicular) rows.

In our work, we (Varian) have struggled with the fact that the terminology of “rows” versus “columns” appears not to be universally (or consistently) defined. In a 96-well plate, passions seem to vary widely about whether a row is defined as running along the long (12-well) or the short (8-well) axis of the plate, or whether you call these directions “across” or “down” (instead of rows or columns). One could also talk

about the “alphabetical” or the “numerical” axis of a plate. Some of these definitions are meaningful only if the orientation of the plate (“portrait” or “landscape” mode) is defined, and this convention also seems to be ill-defined. In this paper we do not attempt to (re-)define any of these terms or conventions; the portrait-style layout of the Gilson liquid handler dictated our initial choice of orientation. We only hope to demonstrate that the ability exists to display NMR data in a variety of formats, each of which offers unique perspectives on the interpretation of these data. It has already been recognized that separate examinations of analytical data aligned along both axes of a plate is a useful tool for the interpretation of other analytical data (like TLC).³¹

Once the data are glued, a user has a choice of displaying the data as either a matrix plot of the entire plate (Figure 3) or in a 2D-NMR style format. The 2D-NMR style format can be plotted as either a contour map (Figure 4) or as a vertical stacked plot (discussed later; Figure 8c,d). The interpretation and utility of Figure 3 is usually self-explanatory, whereas Figure 4, which is different but equally powerful, is sometimes confusing for the uninitiated. The horizontal (F2) axis in Figure 4 displays the ^1H chemical shift, while the vertical axis represents the spectra from wells

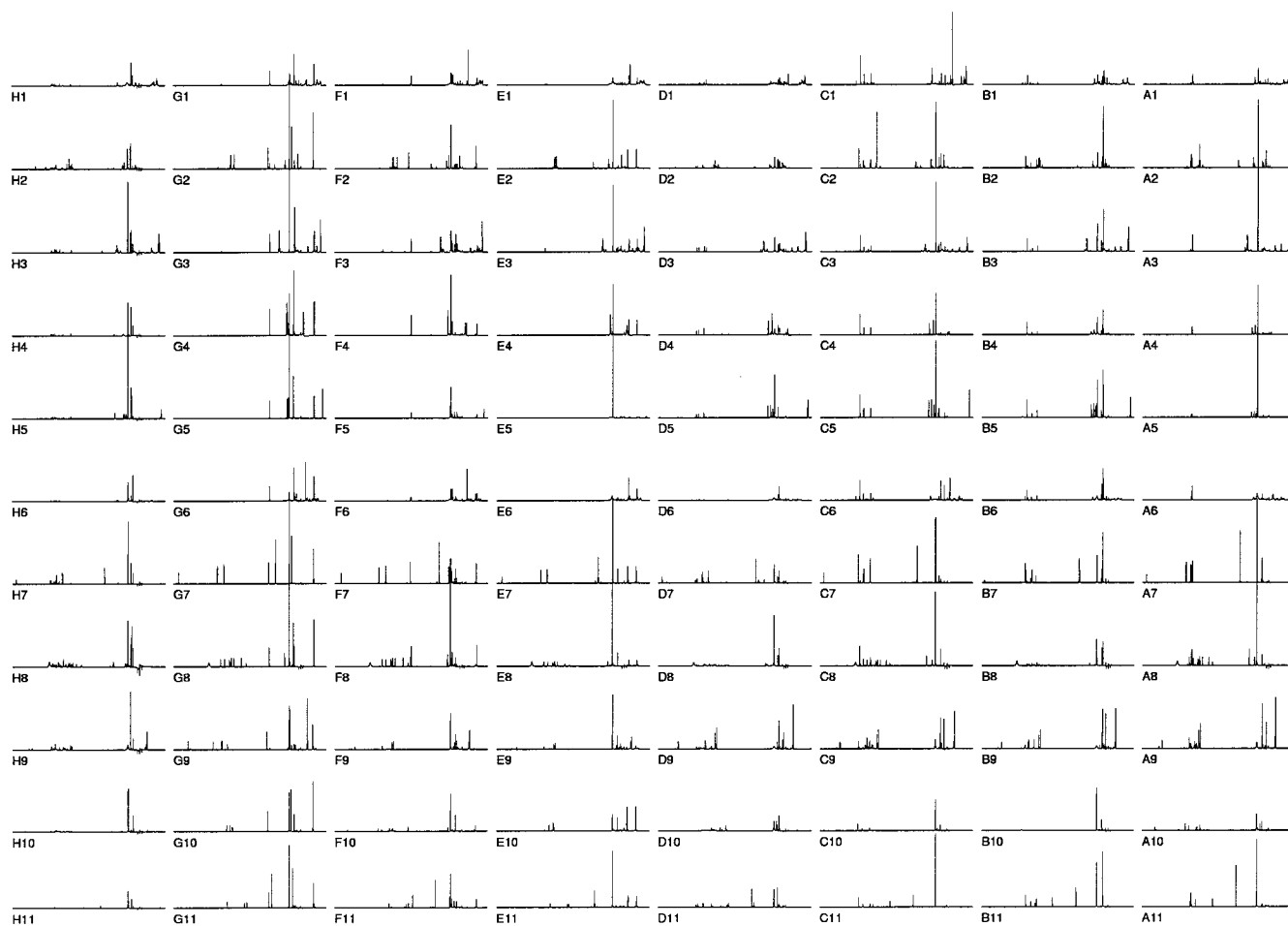


Figure 3. An 8×11 matrix plot of the 88 one-dimensional ^1H NMR spectra acquired on the 25 mM DMSO- h_6 plate. This represents one way to plot the data from an entire titer plate on one page. The position of each spectrum represents the corresponding position of each sample in the microtiter plate; each spectrum is also labeled with its alphanumeric position coordinates. Each spectrum was acquired, processed, and plotted with identical parameters. The entire proton spectrum (0.7–11.2 ppm) is displayed. Although the data presentation differs, these data are identical to the data shown in Figure 4.

1 through 88 (or 96), stacked up in order. This presentation allows one to quickly and simultaneously scan all spectra within the plate for characteristic patterns in the chemical shifts. Both figures (Figures 3 and 4) display the same data, and both presentations have characteristic utilities, strengths, and weaknesses. The matrix plot tends to emphasize patterns in peak intensities and is uniquely capable of displaying spectral patterns along two axes simultaneously. It is also a good format for verifying injection performance (as discussed below and in Figure 16). On the other hand, the 2D contour plot tends to emphasize subtle chemical shift changes (but not intensities) and tends to emphasize relationships and trends along only one plate axis at a time (although that axis can be selected as discussed below).

Although a matrix plot that shows a wide spectral width may be useful for permanently documenting the data from an entire titer plate on only one page (Figure 3 displays a 10.5 ppm spectral width), it does not facilitate any detailed spectral interpretations. The data interpretation usually becomes more difficult as the frequency range of the plot is increased, especially if this wider spectral width includes large resonances (from either unusually strong aliphatic resonances or water). Figure 5, which displays only a 3.2 ppm spectral width, illustrates that a narrower spectral width

makes it easier to see the chemical shift patterns in a matrix plot. If desired, integral traces can also be added to the matrix plot (see Figure 16a).

The NMR data shown here were used, along with LC-MS and TLC data, to determine that some of the reactions did not go to completion. Figure 6 shows the aromatic regions of the proton NMR spectra of the samples located in the “C” column wells (wells C1 through C11; products $4\{3,1-11\}$) of the 2.5 mM DMSO- h_6 plate. This stacked plot was quickly extracted from the fully processed data for the entire plate (using a template generated by the “plateglue” software described later and shown in Figure 9c,d). All 11 spectra can be directly and quantitatively compared. Such a plot is useful for quickly determining either the reaction cleanliness or yield in a series of wells. This figure (Figure 6) shows the reaction of a cyclic anhydride $1\{3\}$ with 11 different primary amines $2\{1-11\}$ (Scheme 2). In these 11 wells, the aromatic resonances of the imide products $4\{3,1-11\}$ were both simple and characteristic (^1H resonances at 7.8 ppm [four-line multiplet], 8.3 ppm [four-line multiplet], and 8.6 ppm [singlet]), and the presence of undesired byproducts was readily apparent by simple inspection of the proton NMR spectra. Hence, we can clearly see that wells C7 and C8 (whose amines contained additional unsaturated

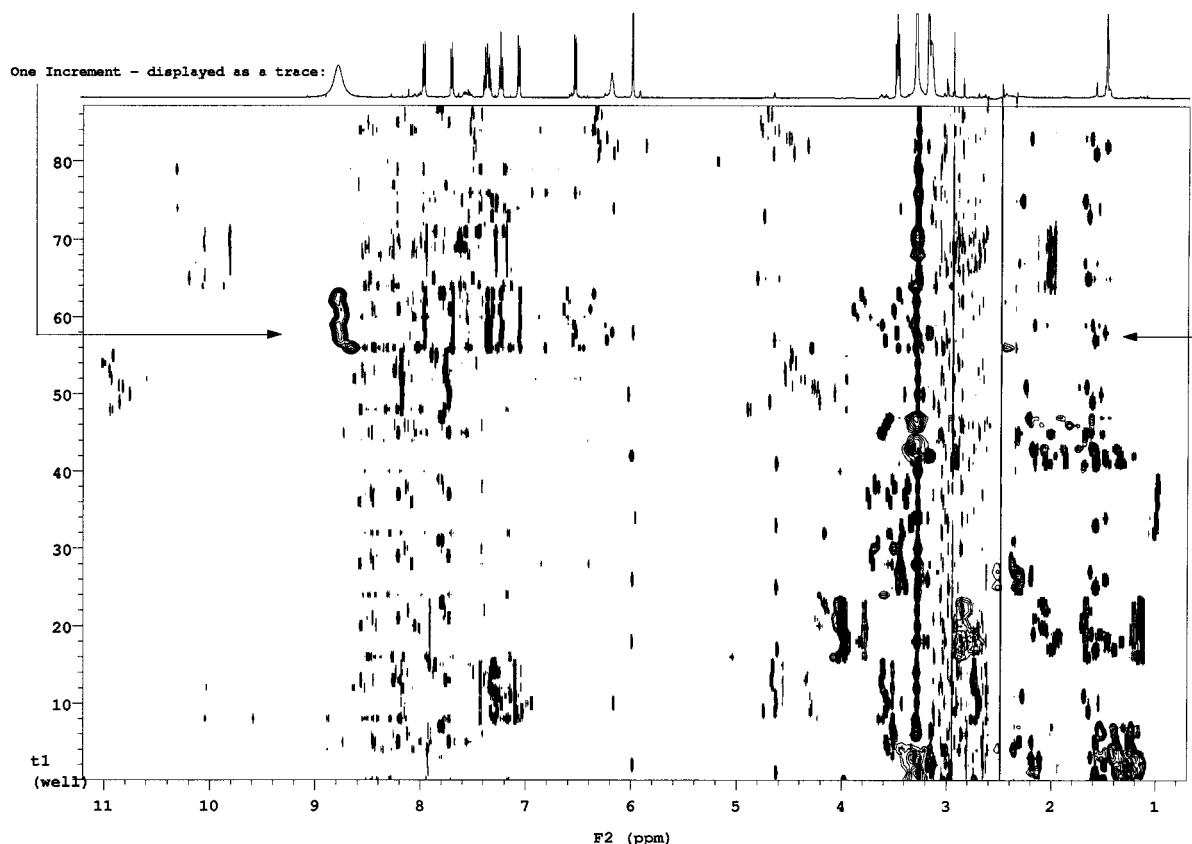


Figure 4. A contour plot of the entire proton spectrum (0.7–11.2 ppm) of all 88 one-dimensional ^1H NMR spectra acquired on the 25 mM DMSO- d_6 plate. This represents an alternative way to plot the data from an entire titer plate on one page. This style of data presentation is especially useful when it can be displayed on the computer screen in an interactive mode. In such a mode, a user can simply slide the cursor up and down the contour display and instantly see the corresponding one-dimensional spectrum for each individual well at the top of the screen. This capability is represented by the conventional plot of the one-dimensional spectrum from well G9 at the top of this figure. Each spectrum was acquired, processed, and plotted with identical parameters. Although the data presentation differs, these data are identical to the data shown in Figure 3.

resonances) contain fairly clean compounds (>90–95%), as do wells C4 and C5 (whose amines did not). Wells C2, C9, C10, and C11 (whose amines had additional unsaturated resonances) contain dirtier products (from 0 to 75% pure), as do wells C1, C3, and C6 (whose amines did not). Wells C1, C5, and C7 exhibit the highest yield of pure compound, wells C2, C3, C4, C6, and C8 exhibit slightly lesser yields (<70%), while wells C9, C10, and C11 clearly exhibit much lower (<25%) yields. Well C9 is a particularly clear example of an incomplete reaction that yielded a number of products and byproducts.

Because this particular reaction does not drastically change the appearance of the aromatic resonances of the cyclic anhydride moiety, it is not easy to distinguish between clean product and clean unreacted starting material from this plot alone. This distinction would be easier, however, if the NMR spectra of the unreacted starting materials were readily available for comparison. This would happen automatically if the starting materials were placed in the wells along the two perpendicular edges of the titer plate and analyzed simultaneously. While this is not a common procedure, its advantages for NMR interpretation are obvious, and we (Alanex) think it will be worthwhile to do this, at least until a database of the ^1H NMR data of all the starting materials (dissolved in identical concentrations in identical solvents) is obtained.

In an analogous manner for a perpendicular set of wells, Figure 7 was used to analyze the eight products contained in wells A7 through H7. These wells contain the products of the reaction of eight different cyclic anhydrides $1\{1-8\}$ with a primary amine $2\{7\}$ that contains resonances at 4–5 ppm (singlet, 2H), 7.8 and 8.2 ppm (doublets, 2H each), and 11 ppm (singlet, 1H). By simple inspection of these well-resolved resonances, especially the amide proton signal at 11 ppm, we can see that wells A7, C7, F7, and G7 each contain a clean compound in high yield, whereas wells B7, D7, E7, and H7 were each the result of unoptimized reactions (since each well contains two or more products, each of significantly lower yield). Similar information can be obtained by examining the 4–5 ppm region and the aromatic region. All this can be gleaned by relatively simple inspection of the spectra, assuming one knows either the starting materials or their corresponding ^1H NMR spectra.

It is useful to have more than one region to examine; notice that the aromatic region of the spectrum from well E7 suggests a clean reaction (and relatively high yield), while the singlets near 4–5 and 11 ppm indicate instead that at least four products have been formed (and a maximum yield of <60% for any one product). In this particular reaction, the chemists determined that it was more correct to analyze the amide proton resonances (near 11 ppm) than the aromatic resonances, because the amide moiety was closer to the

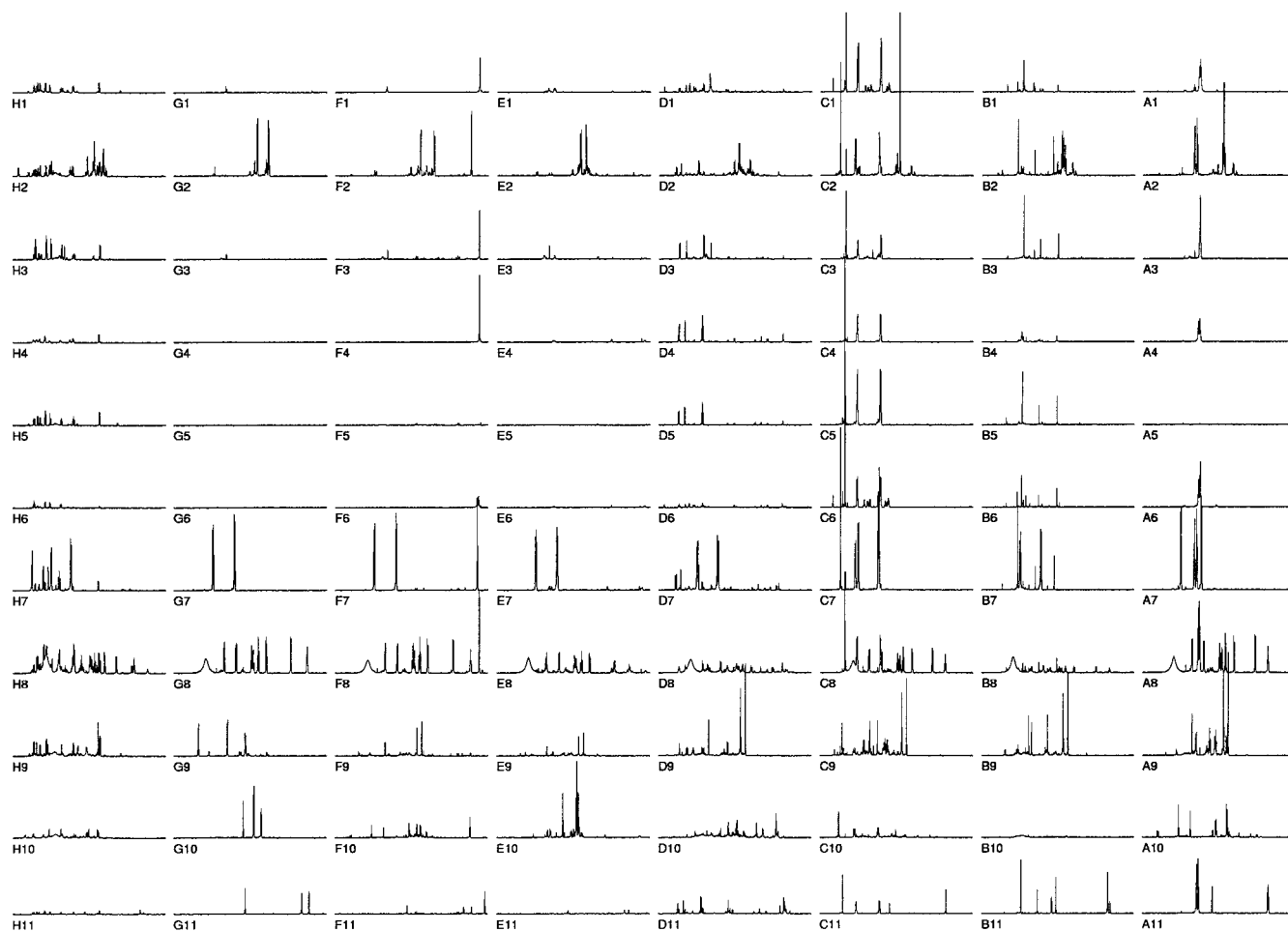


Figure 5. An 8×11 matrix plot of the 88 one-dimensional ^1H NMR spectra acquired on the 2.5 mM DMSO- h_6 plate. This figure contains only a portion of each proton spectrum (the 5.8–9 ppm region). This facilitates detailed interpretations of the data, although all of the NMR data from an entire plate is no longer represented on one page. Each spectrum was acquired, processed, and plotted with identical parameters, and labeled with its alphanumeric coordinates.

reaction center. The same argument could be made for the singlet methylene resonances located at 4–5 ppm, but in some cases their ^1H resonances are less isolated (for example, wells G7 and F7 contain additional resonances from the other reactants) and this makes them more difficult to inspect.

We found during this study that different data-presentation formats can change the way one views and analyzes data. A useful way to illustrate this is to take the same subset of data and present it a number of different ways, as is done in Figures 8 through 12. No single presentation format is superior to another. A careful examination of each figure, however, shows that each different data-presentation format allows different (but mutually compatible) information to be obtained.

Each of the different figures shown in Figures 8–12 are a different representation of the same set of NMR data; that is, the 9.7–11.1 ppm region of the ^1H NMR data acquired on each of the 88 wells in the 2.5 mM DMSO- h_6 titer plate. In Figures 8, 9, and 10, the left-most plots were assembled serially (from well 1 through 88) in groups of eight wells at a time across the short (“alphabetical”) axis of the plate, while the right-most plots were assembled in groups of 11 wells at a time across the long (“numerical”) axis of the plate. If the left-hand plots are said to emphasize the row relationships within the plate, the right-hand plots would then be said to

emphasize the column relationships (depending upon the orientation of the plot, as discussed above). The contour plot in Figure 8a shows that all of the 10.7–11.0 ppm resonances arise from compounds found in only one clustered group of wells (wells 49–56) and nowhere else. It is hard to say, however, if all eight wells contain this resonance, due to the tight clustering in the plot. In contrast, the contour plot shown in Figure 8b, in which the same data are assembled serially across the other axis of the titer plate, clearly shows that all eight wells do contain this resonance. Furthermore, Figure 8b more easily shows that at least several of these eight wells contain multiple resonances in this 10.7–11.0 ppm region (which demonstrates that these wells do not contain pure compounds).

The contour plots (Figure 8a,b) are good at emphasizing row or column relationships, whereas the stacked plots (Figure 8c,d) are better at showing relative peak heights. This is clearly evident, for example, in Figure 8d, which easily shows the peak heights of the minor resonances in relationship to the each major resonance. Figure 8c shows that many of the resonances at 10.05 ppm are actually quite small, and shows that none of the wells in the first half of the plate contain compounds with resonances between 10.3 and 11.1 ppm. (In any of these plots, expansions along either the vertical or the horizontal axes can be made, although no plots

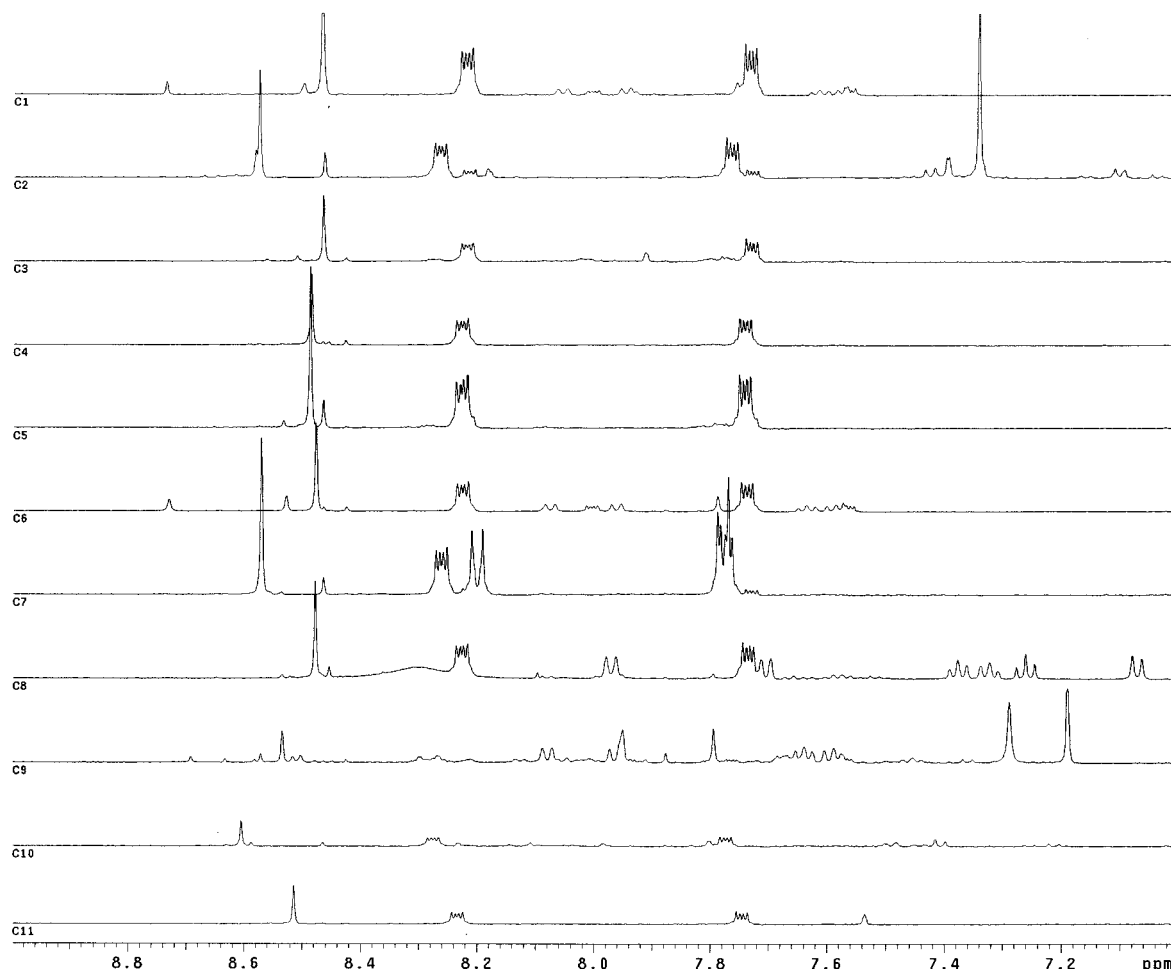
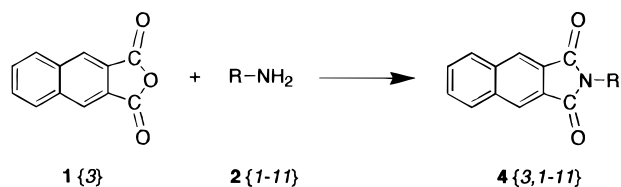


Figure 6. A stacked plot of the proton spectra (7–9 ppm) acquired on the “C” wells (wells C1 through C11—top to bottom) of the 2.5 mM DMSO-*d*₆ plate. This represents the library members produced from the reaction of one cyclic anhydride **1** with 11 different primary amines **2** (products **4**{3,1–11}; see Scheme 2). Each spectrum was acquired, processed, and plotted with identical parameters.

Scheme 2



with an expansion along the vertical axis are shown here. Spectra from wells in selected rows or columns in the titer plate can also be plotted or displayed; Figures 6 and 7 are but two simple examples of this capability.)

In a similar way we can use these plots to analyze resonances at 9.84 ppm. Figure 8a shows that the 9.84 ppm resonances all arise from one “alphabetical” set of eight wells (wells 65–72), but it requires the use of Figure 8b to clearly show that only seven of the eight wells contain this resonance.

Figures of the type shown in Figure 9a,b, called “matrix plots”, provide a more intuitive (graphical) correlation between the NMR data and the layout of the plate. We can see that wells A7–H7 contain the 10.7–11.0 ppm resonances (which are the tallest peaks on the left-hand side of the plotted spectral width) while wells A9–H9 contain the 9.84 ppm resonances (which are the tallest peaks on the right-hand side of the plotted spectral width). Wells A7, C7, G7,

and to a lesser extent F7 exhibit fairly clean singlet resonances at 10.7–11.0 ppm (and so look like fairly pure compounds), while wells B7, D7, E7, and H7 all appear to contain multiple components. This is the same conclusion arrived at by examination of Figure 7, but it was accomplished by looking at patterns in the data from the entire plate (as one might do in an initial survey-mode examination of the plots). Likewise, by focusing on the 9.84 ppm resonances in wells A9–H9, we can see that wells A9, B9, C9, and D9 have a high yield of the compounds that contain this resonance, while wells E9, F9, and H9 contain less than half this amount. Well G9, which is second from one side, does not contain a compound with this resonance (its tall signal is actually at a different chemical shift).

Although Figure 9a allows the peak amplitudes to be compared more easily, Figure 9b—like Figure 8b—allows the peak frequencies to be compared more easily. The data are the same, only the rotation of the plot differs. (A closer examination of Figures 9b, 9a, 8d, and 8b suggests that the 9.84 ppm resonance expected for well G9 has been shifted downfield to 10.2 ppm and that it exists in high yield. This hypothesis could only be answered by studying the reaction chemistry for that well in more detail.)

To facilitate both the gluing and the redisplay of wells in different orders (as was used in the preceding figures) we

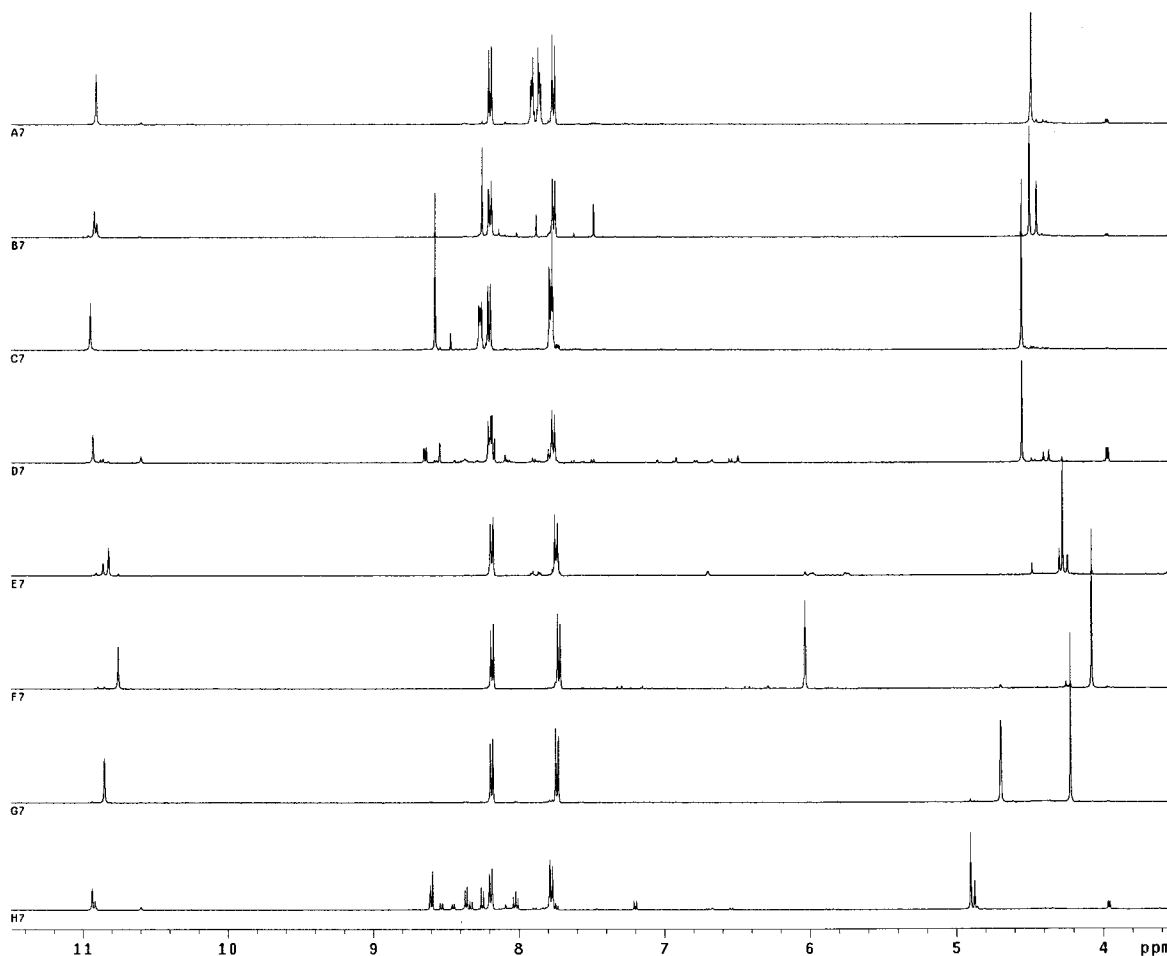


Figure 7. A stacked plot of the proton spectra (3.5–11.5 ppm) acquired on the “7” wells (wells A7 through H7—top to bottom) of the 2.5 mM DMSO- h_6 plate. This represents the library members produced from the reaction of eight different cyclic anhydrides **1** with one primary amine **2** (products **4**{7,1–8}). Each spectrum was acquired, processed, and plotted with identical parameters.

developed the software tool called “plateglue” which is shown in Figure 9c,d. By using a computer mouse to select wells (or rows of wells) in a specific order, a template is created which can be used to define either the glue order or the display order of the spectra in any plate. Following the convention established in the preceding figures, Figure 9c shows the software defining that the spectra will be assembled along the “alphabetical” axis, while Figure 9d shows the software defining a “numerical” axis assembly. Figures 6 and 7 (as well as other similar plots and displays) were also created with this tool by creating single-row or single-column templates.

In contrast to the preceding figures, which display the spectral data, Figures 10, 11, and 12 are displays of the corresponding integral information (from the same data set). Figure 10 is a graphical representation of the integral intensities for a particular frequency range for all 88 wells at once. Since this plot uses the matrix format, it is very easy to quickly scan the data for trends in quantitation. (The integral can be plotted either with the spectral data, as is shown in Figure 16a [discussed below], or without, as shown here. Although the accuracy and precision of integral data in VAST have not yet been evaluated, quantitation data for another flow NMR technique—FIA-NMR—has recently been measured.²⁵) Once these integral regions have been defined, it is possible to write this integral information to a text file

(Figure 11a). This text file can be used alone, or it can be imported into a personal computer spreadsheet (Figure 11b). Even more interesting is to import these data into another software tool we developed, called “combiplate”, that displays numerical information as a color density (Figure 12). This use of color facilitates a rapid visual quantitative comparison of the data (in this case, the 9.7 to 11.1 ppm integral intensities for each well in the plate). Figure 12 uses the same data that was displayed in Figures 8–11 but presents it in a manner that is both new and novel to NMR spectroscopy. (The use of color to help “mine” mass spectral data has recently been shown.³²)

The combiplate displays shown in Figure 12 can be compared to the table of integral values shown numerically in Figure 11b. Figure 12a, which uses the dynamic range of only one color and is normalized to the maximum integral value, visualizes wells whose integral values range from a low of 9 to a high of 84 (the maximum). Figure 12b, which also uses only one color but with the color intensity scaled so as to emphasize smaller integral values, differentiates wells whose integral values range from a low of 3 to a high of 23. Figure 12c illustrates the use of combining the colors shown in Figure 12a,b to achieve a wider dynamic range of information. All of the integral intensities ranging from 3 up to 84 can be observed and discriminated; the shades of

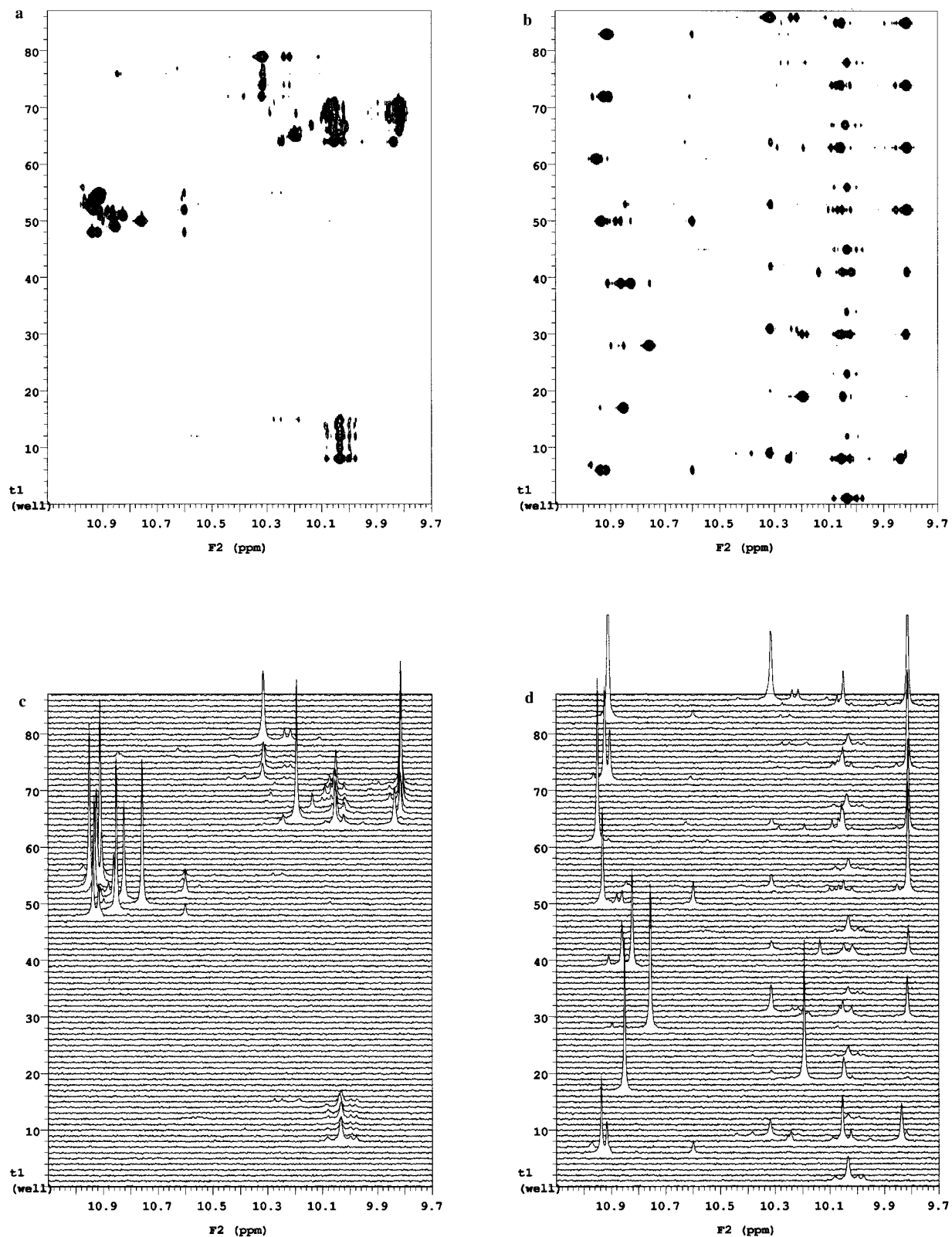


Figure 8. Four different representations of the same NMR data, acquired on the 88 library members in the 2.5 mM DMSO- h_6 plate. Each plot emphasizes different aspects of the data and allows different questions to be answered. The contour plots on the top (8a and 8b) emphasize pattern relationships, while the stacked plots on the bottom (8c and 8d) facilitate more quantitative comparisons. The plots on the left (8a and 8c) were “glued” in groups of eight along the short axis of the titer plate, while the plots on the right (8b and 8d) were “glued” in groups of 11 along the long axis of the plate. For comparisons, see Figures 9–12. For clarity, only the NH region at 9.7–11.1 ppm is shown here.

green reflect the range of smaller integral values, while the shades of white reflect the range of larger integral values.

In addition to the example shown in Figure 12, combiplate can also be used to make Boolean logic queries (display the

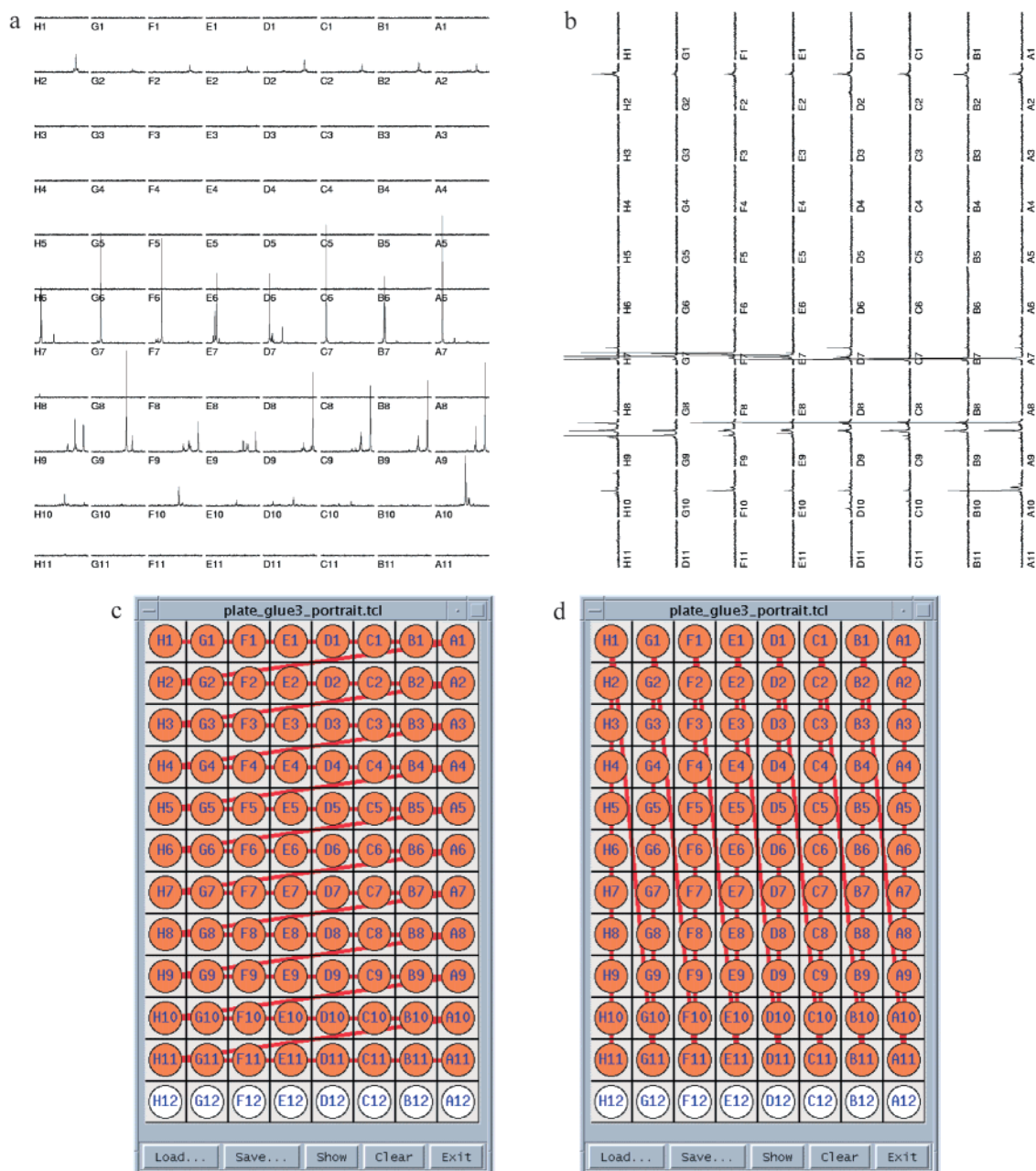


Figure 9. The matrix plots on the top are two more different representations of the NMR data shown in Figure 8. The matrix plot on the top left (9a) was “glued” in groups of eight along the short axis of the titer plate, while the matrix plot on the top right (9b) was “glued” in groups of 11 along the long axis of the plate. For comparisons, see Figures 8 and 10–12. For clarity, only the data from the NH region at 9.7–11.1 ppm is shown here. The lower half of this figure shows how the “plateglue” software can be used to define the gluing or display pattern. Figure 9c represents the format used to create Figures 8a and 8c, while Figure 9d shows the format used to create Figures 8b and 8d.

methoxy integrals in red and the NH integrals in green). It can display peak heights or integral areas of an internal standard, which helps in quantifying or verifying the sample injections of an entire plate, as is shown in Figure 16b (discussed below). Combiplate is a general tool that can be used to represent any type of numerical data, including direct numbers (NMR peak height, bioassay activity, compound mass, etc.), ratios of numbers (the ratio of a compound’s integral area to the integral of an internal standard, as would be used to calculate a quantitative yield), or differences from an average (to verify reproducibility).

Two additional questions we hoped to answer during this study were (1) could usable data be acquired from samples

dissolved in protonated (rather than deuterated) DMSO, and (2) what concentration of sample was needed? If nondeuterated solvents could be used, this would allow the same titer plate to be used for other analyses (including mass spectrometry) and would also reduce the cost of the analysis. If the required sample concentration could be kept low, problems that might arise from limited solubility or sample precipitation could be reduced. (Additional experimental issues—such as what is the minimal sample volume, and how fast can the analysis be run—will be covered elsewhere.)

To help answer these questions, we acquired NMR data on three different plates of our 88-member library, each of which had been reconstituted in one of three different

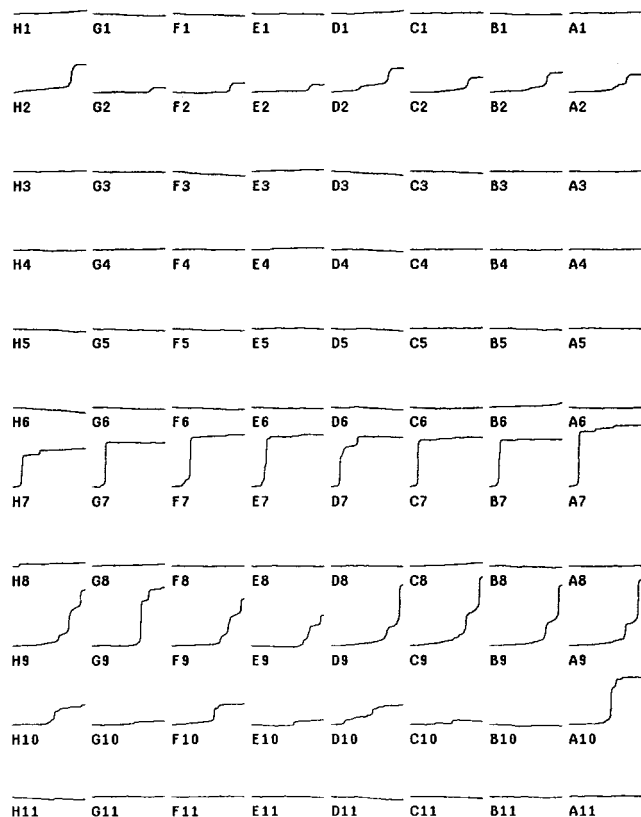


Figure 10. Another representation of the data shown in Figures 8–9 and 11–12; this time a matrix plot of the integral region for each well. Again this displays information on the same NH region at 9.7–11.1 ppm for the 88 library members in the 2.5 mM DMSO- h_6 plate. One can immediately see that the “7s” and “9s” (wells A7 through H7, and A9 through H9, respectively) possess the largest NMR integrals, while the “2s” and the “10s” possess smaller integrals. The integral area for well A10 seems anomalously large, while the integral for well E9 seems anomalously small. For comparisons, see Figures 8–9 and 11–12.

ways: 25 mM in DMSO- h_6 , 2.5 mM in DMSO- h_6 , and 2.5 mM in DMSO- d_6 . Side-by-side comparisons of the three data sets are shown in Figures 13, 14, and 15. (Figure 2 was also prepared from these data sets.) The data from all three data sets look equally good, which indicates that any of the conditions (25 mM or 2.5 mM; DMSO- d_6 or DMSO- h_6) can be used to acquire data with VAST. (Of course a 25 mM spectrum will always have better signal-to-noise than a 2.5 mM spectrum, and this will always facilitate the observation of minor components in impure samples.) Virtually all of the significant differences between these three data sets are located in the region around the DMSO solvent resonance and are caused by solvent suppression (Figure 15). The ability to see signals underneath the solvent resonances is dependent upon both the NMR acquisition parameters (i.e., the shape and the bandwidth of the selective WET pulses) and the NMR processing parameters (i.e., the parameters controlling the software DSP solvent-suppression notch filters).

Examples of some of the few observable differences are highlighted in Figure 15. Arrow **a1** indicates a resonance that is visible in all three data sets, even though it is almost underneath a ^{13}C satellite of the DMSO. Arrow **b2** indicates a resonance that, like signal **a1**, is also essentially underneath

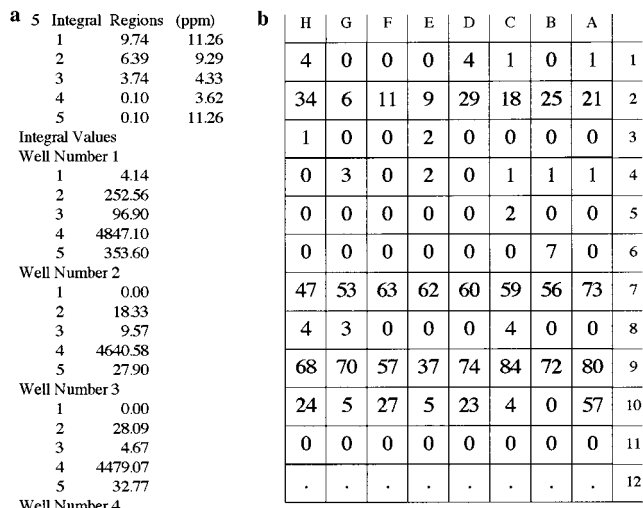


Figure 11. Two additional (different) representations of the integral data shown in Figures 10 and 12. Again this displays information on the same NH region at 9.7–11.1 ppm for the 88 library members in the 2.5 mM DMSO- h_6 plate. The leftmost display (Figure 11a) shows the initial portion of a text file written to disk by the VNMR software. The header of the file shows the frequency limits for each integral region. The rest of the file shows the integral area for each of the integral regions for each well in the plate. In the display on the right (Figure 11b), the integral values from the first integral region (from 9.74 to 11.26 ppm) have been imported into a spreadsheet from the file shown in 11a. This allows the numerical data to be redisplayed in a matrix format.

the ^{13}C satellites of the DMSO- h_6 samples; however, this one is visible in the 25 mM and the DMSO- d_6 spectra, but not in the 2.5 mM DMSO- h_6 spectrum. Arrow **c3** points to a cluster of resonances that are different in all three spectra, with the 2.5 mM DMSO- h_6 data again providing the least amount of information. Arrow **d4** indicates a resonance in which this difference is even more pronounced. Arrow **e5** points to an area in which the 2.5 mM DMSO- d_6 spectrum contains more data than either the 25 mM or (especially) the 2.5 mM DMSO- h_6 spectra. Arrow **f6** points to a signal that is only visible in the spectrum run in deuterated solvent.

The spectral “ridges” that run vertically in Figure 15 (along the entire length of the spectra) are caused by either solvent impurities or residual solvent resonances. The ridge at 2.5 ppm is caused by the main resonance of DMSO, while the ridges at 2.36 and 2.64 ppm (left and middle spectra only) are caused by residual signals from the suppressed ^{13}C satellites of the DMSO- h_6 . The ridge at 3.5 ppm is from water that has been absorbed into the DMSO. The ridges at 1.1 and 1.2 ppm (a triplet and a singlet, respectively), as well as the smaller ridge at 2.95 ppm (singlet), are due to impurities in the DMSO- h_6 .

This illustrates that solvent purity can have a significant impact upon data quality. All solvents can absorb atmospheric water, which adds an additional (often broad) resonance into the proton spectrum, but DMSO is especially problematic because it is very hygroscopic. The resonance frequency of water in DMSO can be present in a wide region—anywhere between 3 and 4 ppm depending upon the amount of absorbed water. This resonance can make solute resonances that are located at the same chemical shift difficult to observe. The SCOUT-scan technique can easily track and

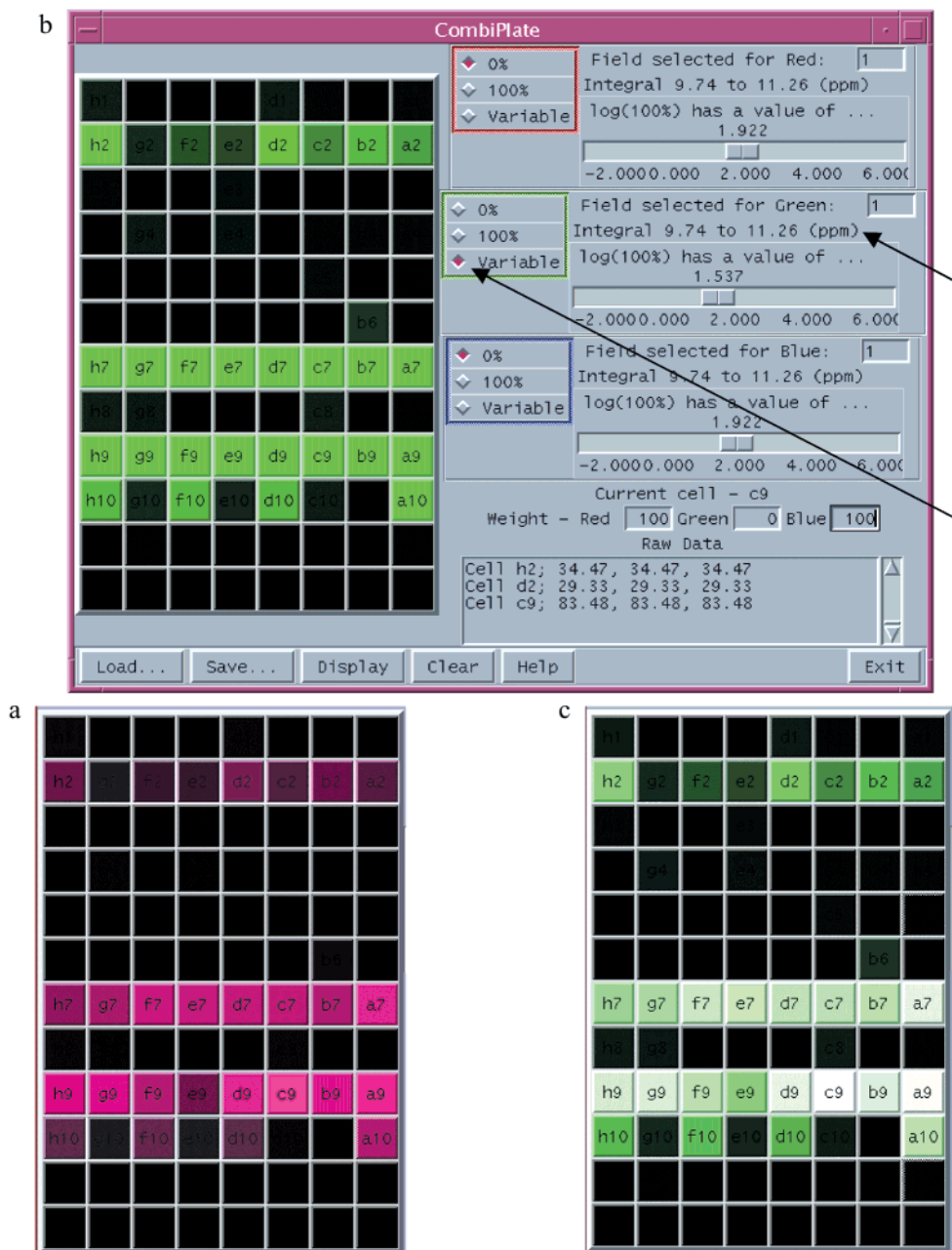


Figure 12. Another form of displaying the integral data shown in Figures 10 and 11. Here the integral intensities are represented by color densities that are arranged in a matrix format. The VNMR software tool (“combiplate”) that generates this display allows three colors to be used to represent different integral regions. The colors can be used in different combinations to illustrate different ways of visualizing data. (All data shown here are from the same NH region at 9.7 to 11.1 ppm of the same 88 library members in the 2.5 mM DMSO- h_6 plate). In Figure 12a, purple is used (red and blue combined); the intensity of the purple was normalized to the well with the strongest response (well C9 had an integral area of 84; see Figure 11b). In Figure 12b, green is used; the intensity of the green was set (with the slider bars) to saturate intensity differences in the “7s” and “9s” row in an effort to better visualize the minor components in the “2s” and “10s” rows. In Figure 12c, the purple and green displays in 12a and 12b are combined to increase the effective dynamic range. The resulting shades of white (produced by the combination of purple and green) represent the integral areas of the highest concentration samples (brighter whites represent larger integrals), while shades of green represent the integral areas of the lowest concentration samples (brighter greens represent larger integrals). This tool can be used to visualize any type of numerical data, including ratios of numbers.

suppress the water resonance (if desired), but both NMR suppression and DSP notch-filter processing can also eliminate those solute resonances that are located at the same chemical shift. One advantage of the notch-filter processing is that it does offer the user a chance to either re-optimize or eliminate its effects long after the data has been acquired. If possible, however, it is always better to try to keep the solvent as dry as possible in the first place so that none of these tools need to be used. (The plates used in this study

were reconstituted and heat sealed with automation equipment, which allowed the DMSO in each well to remain relatively dry; however, the water still ended up being the largest peak in every spectrum.)

Other impurities in the solvent can also be an issue. We have struggled with this problem in LC-NMR for some time, where even 0.01% impurities in the solvents are detectable. As shown in Figure 15, these impurities will appear in a contour plot as a long ridge that complicates the analysis.

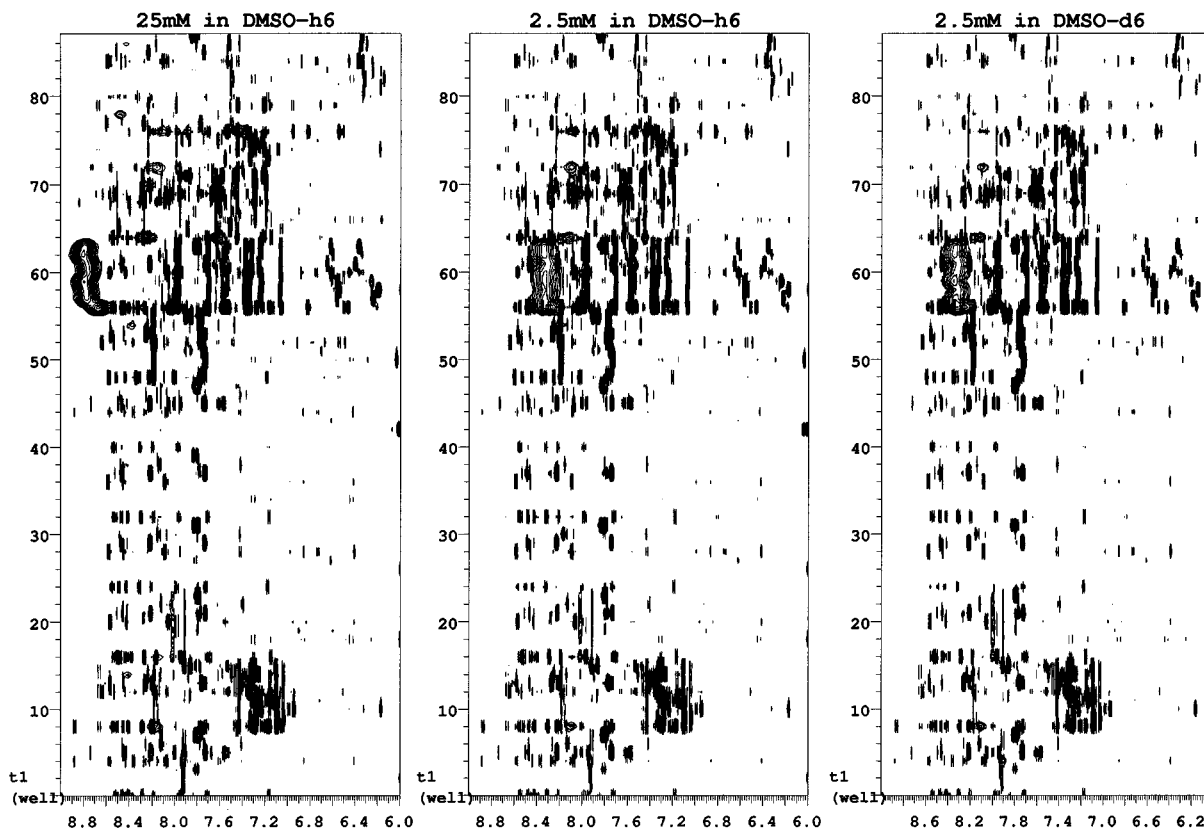


Figure 13. A comparison of the 6–9 ppm regions from the 25 mM DMSO- h_6 data set (left), the 2.5 mM DMSO- h_6 data set (middle), and the 2.5 mM DMSO- d_6 data set (right), shown as contour plots. The identical appearance of each plot shows that all three conditions (25 mM or 2.5 mM; DMSO- d_6 or DMSO- h_6) can be used to acquire VAST data. Note, however, that some broad anilide NH resonances exhibit a different chemical shift in the 25 mM spectrum (8.8 ppm) than in the 2.5 mM spectra (8.4 ppm). Single-frequency WET solvent suppression and DSP notch filters (ssfilter) were used to acquire the DMSO- h_6 data (left and middle), but not the DMSO- d_6 data (right). The 25 mM data were plotted with a 10 \times lower vertical scale to facilitate intensity comparisons with the 2.5 mM data sets. All data acquisition, processing, and display parameters were otherwise the same for all three plots.

We have found that all of the commercial grades of DMSO- h_6 we have studied (including glass-distilled grades) exhibit an additional resonance at 2.9 ppm. The intensity of this signal is variable, depending upon the grade and supplier of the solvent; however, it is not present in DMSO- d_6 . It has been proposed that this resonance is due to the presence of dimethyl sulfone that is created by the autodissociation of DMSO into dimethyl sulfide (which is volatile) and dimethyl sulfone.³³

During the analysis of our first batch of plates in this study, we detected a constant set of unknown resonances that were present in every well. Because these resonances were present in every well at the same concentration, we assumed that they were unrelated to the compounds (or the chemistries) used to make the library members themselves. These resonances (a doublet at 3.12 ppm [$J = 5.2$ Hz] and a corresponding quartet at 4.05 ppm) were subsequently identified as belonging to methanol dissolved in the DMSO. This methanol impurity was tracked down as being introduced via the DMSO solvent that was used to reconstitute the dried compounds in each well of the plate. As a consequence, the manufacturing step that unnecessarily introduced this methanol into the DMSO-dilution equipment was discontinued for all subsequent microtiter plates (at least those destined for NMR analysis).

At this point we have demonstrated that the capability to acquire one-dimensional ^1H NMR data on every member of

a combinatorial library now exists and has become essentially routine. Now the questions are what do you do with all the data, and what does a chemist hope to get by having all this NMR data? Already, many combinatorial-chemistry programs routinely obtain mass spectrometry and HPLC-UV (photodiode-array detection) data on all their samples. They would like to use NMR as a “universal” detector—preferably as one that does not require an HPLC “front end”—as a method to see all the products, as neither MS or UV are universal detectors. (Of course all methods have their limitations; ^1H NMR cannot detect the presence of inorganic salts.) The simplest way to deal with the mass of information is to merely archive all of the NMR data in an electronic database (without interpretation) for long-term documentation purposes. This goal can be fully realized now, although some groups (justifiably) question whether this use alone can justify the expense and effort of obtaining NMR data. The second goal is to use this NMR data to confirm the suspected structures of each library member. This can be accomplished today by using manual (and laborious) interpretation of each spectrum by the chemist, although the capabilities of computer-assisted structural assignments software are rapidly improving.³⁴ The third goal is to use the NMR data to assess compound purity, while the fourth goal is to determine yield. Assessing compound purity requires detailed information about chemical-shift assignments, but yield measurements can be used instead to place an upper boundary on the purity.

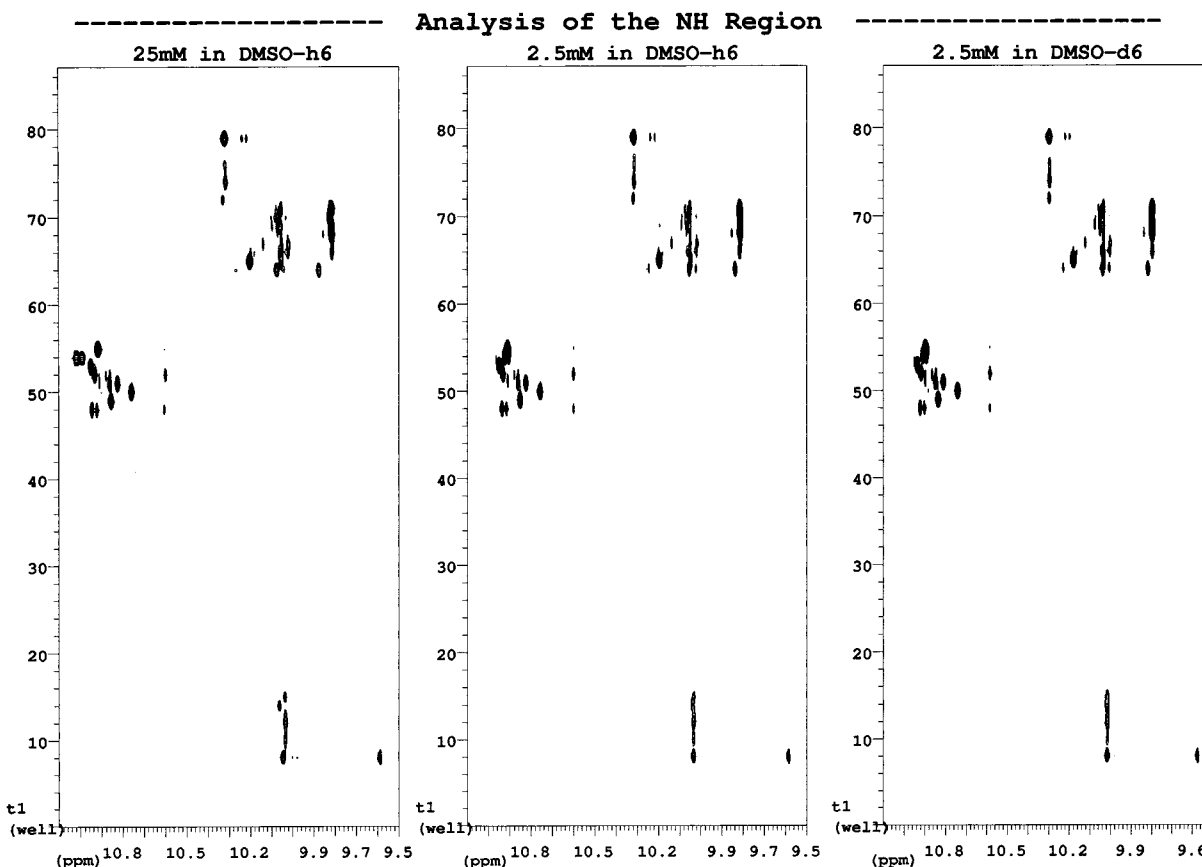


Figure 14. A comparison of the 9.5–11 ppm regions from the 25 mM DMSO- h_6 data set (left), the 2.5 mM DMSO- h_6 data set (middle), and the 2.5 mM DMSO- d_6 data set (right), shown as contour plots. The identical appearance of each plot shows that all three conditions (25 mM or 2.5 mM; DMSO- d_6 or DMSO- h_6) can be used to acquire VAST data. Single-frequency WET solvent suppression and DSP notch filters (ssfilter) were used to acquire the DMSO- h_6 data (left and middle), but not the DMSO- d_6 data (right). The 25 mM data were plotted with a 10 \times lower vertical scale to facilitate intensity comparisons with the 2.5 mM data sets. All data acquisition, processing, and display parameters were otherwise the same for all three plots.

Yield measurements typically use internal standards for comparisons; however, some chemists are excited about the potential of doing quantitation just by plotting the integral intensity of a particular chemical-shift range in the 96-well (matrix) format (Figure 10). The relative importance of determining either the purity or the yield will depend on the intended final use of the product. Reaction optimization groups probably consider yield information more important than purity, whereas bioassay groups are probably more concerned about purity.

Clearly, the data analysis stage has now become the biggest stumbling block in the entire process, and the need for better automated data analysis tools should present an engaging challenge to the computational groups of the world. Already, there are tantalizing developments being made in the fields of database matching and spectral prediction,³⁴ Bayesian spectral analysis,^{35,36} spectral simplification,³⁷ and filter diagonalization methods (FDM),^{38–40} among others. The FDM method in particular offers significant possibilities for reducing data acquisition times and data storage requirements. Clearly, all aspects of this field of combinatorial chemistry are still evolving, and additional techniques for the automated computer analysis of VAST spectra are in development.

A second area of potential growth is the analysis of mixtures. If a particular reaction yields a variety of products,

it would be useful to identify each of the products. In addition, a common way to speed up any analysis is to make it parallel, and one way to attempt this in NMR is to purposely analyze mixtures.^{41,42} By definition, mixture analysis requires some means of resolving the individual components. Although this is typically done with some form of chromatography, some spectroscopic methods do exist. Chromatographic separations can be accomplished using either traditional off-line fractionation prior to the NMR analysis, or with on-line fractionation as is used in LC-NMR.⁴³ Spectroscopic methods for analyzing mixtures include diffusion-ordered spectroscopy,^{44,45} relaxation-edited spectroscopy,⁴¹ diffusion-edited “affinity NMR”,⁴² isotope-filtered affinity NMR,⁴⁶ diffusion-ordered TOCSY,⁴⁷ and SAR-by-NMR.⁴⁸ It is also appropriate to recognize that a one-dimensional proton NMR spectrum, which separates nuclei into groups of discrete resonance frequencies with integratable signal intensities, by itself affords a certain degree of mixture analysis.

A third area of potential growth is the increased use of NMR for quantitation. Alanex currently uses internal standards to determine both yield and/or purity in their samples analyzed by NMR and expects to continue this practice with VAST. (Previously they used TLC to analyze sample purity; now MS and HPLC supplant this, soon to be followed by NMR data.) Internal NMR standards which can (or have)

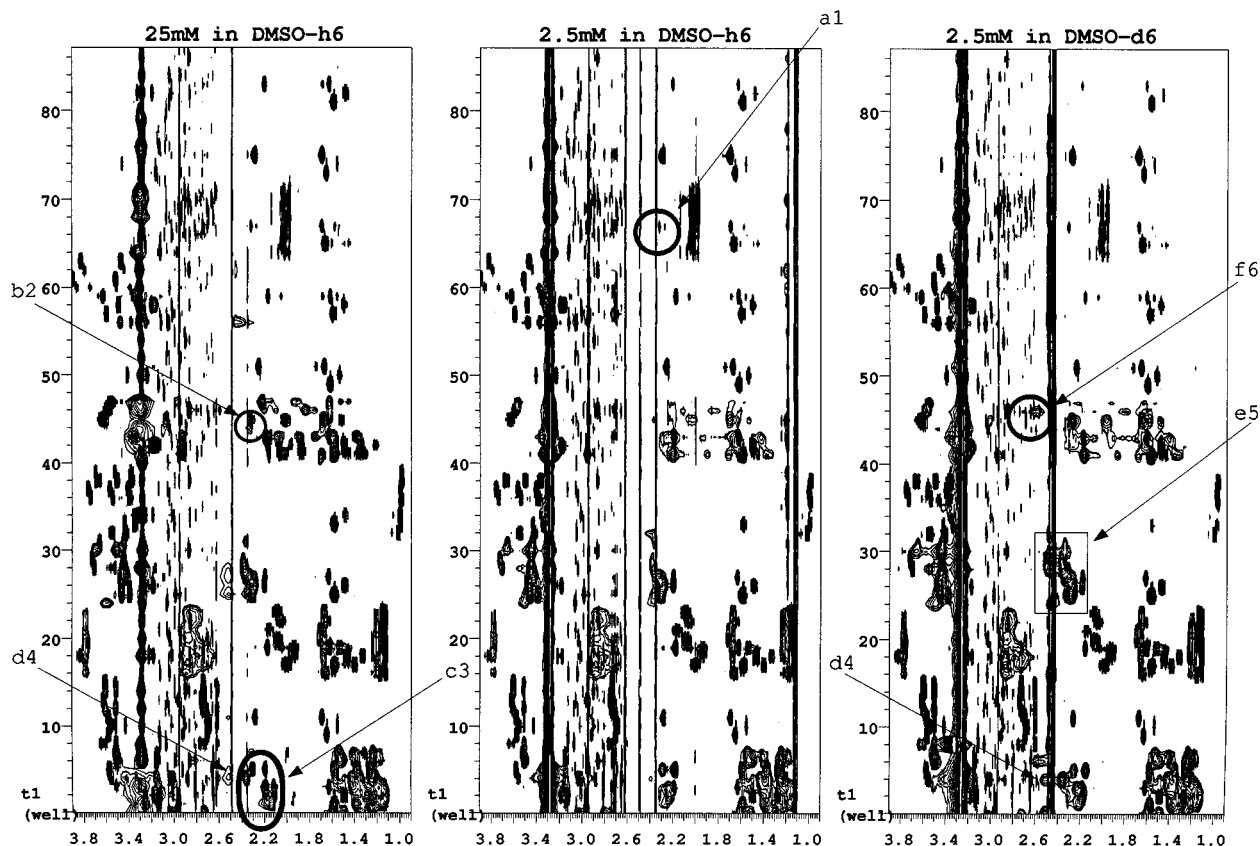


Figure 15. A comparison of the 0.9–3.9 ppm regions from the 25 mM DMSO- h_6 data set (left), the 2.5 mM DMSO- h_6 spectrum (middle), and the 2.5 mM DMSO- d_6 spectrum (right), shown as contour plots. The arrows, circles, and boxes indicate regions of special interest for comparison purposes (see text). Single-frequency WET solvent suppression and DSP notch filters (ssfilter) were used on the DMSO- h_6 spectra (left and middle), but not on the DMSO- d_6 spectrum (right). The 25 mM data were plotted with a 10 \times lower vertical scale to facilitate intensity comparisons with the 2.5 mM data sets. All data acquisition, processing, and display parameters were otherwise the same for all three plots.

been used by Alanex include tetramethylsilane (TMS), hexamethyldisiloxane (HMDS), 1,3,5-trichlorobenzene, 1,3,5-trimethoxybenzene, *p*-dimethoxybenzene, and 2,2,3,3-tetramethylbutane. As expected, the integrity of the integral areas of an internal standard decreases if the NMR repetition rate is short compared to the proton T1 value. Clearly, all the usual precautions for acquiring quantitative NMR data should be observed if purity and yield information are to be obtained. We (P.A.K.) have also observed that for identical resonances in equimolar-concentration solutions, the T1 values can vary depending upon whether the samples were dissolved in DMSO- d_6 or DMSO- h_6 .

An additional advantage of using an internal standard in DI-NMR is that an inspection of one of the internal standard's resonances (especially a sharp singlet) can serve as a quality control check of the integrity of the sample-injection, shimming, and NMR-acquisition processes. An example of this is shown in Figure 16. These data contain information about the singlet resonance from an internal standard dissolved at constant concentration in every well of the plate. Two different representations of the data are shown. The data presentation on the left (Figure 16a) superimposes three bits of information. First, it uses alphanumeric labels to show the spatial position of each spectrum (i.e., how each spectrum maps to a distinct position within the plate). Second, each spectrum conveys information about the NMR resolution and line shape obtained on the sample

in that well. This helps monitor both the integrity of the sample and the injection (e.g., a lack of air bubbles and particulates in the flow cell, and a sufficient sample volume) and the reliability of the gradient shimming, since any such deficiencies will cause a distorted line shape. Third, the consistent height of the superimposed integral trace is further verification that both the quantity of injected sample and the NMR acquisition were reproducible. (Monitoring the integral area by itself may be insufficient since additional coincident resonances could alter the integral area. Monitoring the peak height by itself is insufficient since it is overly sensitive to small changes in T1 and spectral resolution. A bad line shape accompanied by a constant integral area, however, would help indicate that a small foreign body is in the flow cell.)

Another method of rapidly visualizing the integral area of an internal standard is shown in Figure 16b. The uniformity of the red color shown for each well is an indication of the uniform quantity of the internal standard. In contrast to Figure 16a, the display in Figure 16b allows a user to more rapidly discern small (5%) changes in the integral areas. Either data presentation mode could probably be improved by also displaying the *difference* of each measured value from its corresponding average.⁴⁹

Finally, the issue of whether the starting materials should be included in the plate and subjected to NMR analysis should be summarized. There are four advantages to doing this. First, it would allow the spectra of the starting materials

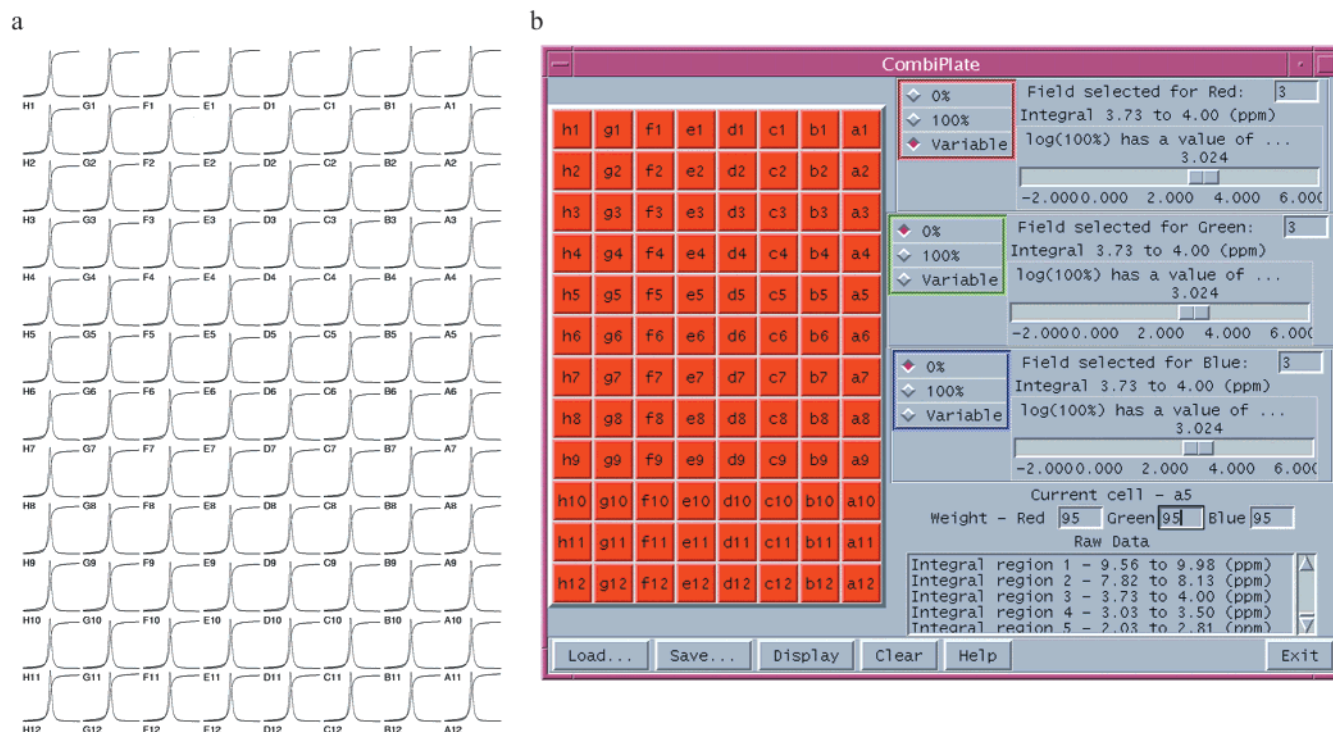


Figure 16. Two different representations of using an internal standard to monitor the reproducibility of NMR automation. The concentration of the internal standard was constant across the plate, as were the NMR acquisition, processing, and plotting parameters. The well-to-well consistency of the data is a measure of the consistency of automated sample injection, gradient shimming, and NMR acquisition. The display on the left (16a) is an 8 × 12 matrix plot that shows the spectrum, the integral, and the corresponding alphanumeric label for each well. The display on the right (16b) is a color-coded representation of the integrals. (All data monitors the same NMR signal arising from the lowest-field *N*-methyl resonance of caffeine dissolved in DMSO-*d*₆. Each spectrum represents a 100 Hz wide region around this 3.83 ppm resonance. Each spectrum was acquired with VAST automation using ¹H gradient shimming and 32 scan acquisitions and was plotted in an absolute intensity mode.)

to be glued together with the spectra of the compounds of interest, and this would facilitate the analysis of the products. Second, this would negate and all solvent-, concentration-, or temperature-dependent effects in the NMR spectrum. Third, these spectra could then be incorporated more easily into a spectral database (to improve the accuracy of the computer-based spectral-prediction software).³⁴ Fourth, these data help evaluate the reactivity of the starting materials with the solvents. If used for this purpose, one needs to decide whether the starting materials should be subjected to the reaction conditions before analysis. If so, then the reactivity of the starting materials, its contaminants, or solvent degradation byproducts of the solvent can also be monitored. Some of the compounds analyzed in this study were found to contain unexpected impurities, which were later shown to arise from reactions with a solvent-degradation byproduct. This was eventually detected and corrected, although the problem could have been solved more readily if the starting materials were also carried through the reaction conditions and then analyzed by VAST.

The analysis of the starting materials, however, has two disadvantages. First, it effectively decreases NMR sample throughput (since it would increase the number of spectra being acquired). Second, if the starting materials are placed in the same titer plate as the products (where they would occupy one row and one column of each plate—a total of up to 19 wells) the resulting plate format (which could then hold only a maximum of 77 “real” samples) would create a format mismatch with most other titer plate applications. This

problem, however, could easily be solved by placing the starting materials in a different plate (or series of vials) for subsequent NMR analysis.

Conclusions

This paper has described our development of a novel technique, which we call direct-injection NMR (DI-NMR), that has proven useful as an automatic sample changer for NMR. Details of our specific implementation of DI-NMR, called VAST, have been described. We have shown that data can be acquired on samples dissolved in either deuterated or protonated solvents, and we have discussed the use of internal standards and NMR quantitation. We have shown how VAST can be used to acquire one-dimensional ¹H NMR data on every member of a combinatorial library. This capability is now becoming routine, both for us and for others.^{50,51} The success of the data-acquisition aspects, however, has made it apparent that data processing is now the next challenge. As a result, we have also presented several new processing and display options that facilitate faster, easier, and more powerful (but manual) analyses of the resulting NMR data. The varieties of display options, some of which are similar to the displays used for 2D-NMR data, are changing how chemists interact with NMR data.

Acknowledgment. The authors are gratefully indebted to Dan Iverson, Greg Brissey, Ron Haner, Chris Kellogg

(all of Varian, Inc.), and Doug Phillipson (Alanex) who have contributed to many aspects of this project, both through software and hardware development and through numerous discussions.

References and Notes

- Presented in part by P. A. Keifer: IBC Symposium "Drug Discovery Technology" (19–22 Aug 1996, Boston, MA, USA – poster 11), Kinki Chemical Society Symposium "Combinatorial Chemistry & High Throughput Screening" (30–31 Jan 1997, Osaka Prefecture University, Osaka, Japan), 213th ACS National Meeting (13–17 April 1997, San Francisco, CA, ORGN-277), IBC Conference on "Miniaturization Technologies (in Combinatorial Chemistry)" (22–24 Feb 1998, Squaw Valley, CA), SRI Symposium "High Throughput Analysis and Purification of Combinatorial Libraries" (27–28 July 1998, Philadelphia, PA), and CHI Symposium "NMR Technologies for Drug Design and Development" (29–30 Oct 1998, Baltimore, MD).
- Gordon, E. M.; Gallop, M. A.; Patel, D. V. Strategy and Tactics in Combinatorial Organic Synthesis. Applications to Drug Discovery. *Acc. Chem. Res.* **1996**, *29*, 144–154.
- Special Thematic Issue of *Chemical Reviews*, **1997**, *97*, 1–508.
- Gallop, M. A.; Fitch, W. L. New methods for analyzing compounds on polymeric supports. *Curr. Opin. Chem. Biol.* **1997**, *1*, 94–100.
- Carrasco, M. R.; Fitzgerald, M. C.; Oda, Y.; Kent, S. B. H. Direct Monitoring of Organic Reactions on Polymeric Supports. *Tetrahedron Lett.* **1997**, *38*, 6331–6334.
- Egner, B. J.; Bradley, M. Analytical Techniques for Solid-Phase Organic and Combinatorial Synthesis. *Drug Discovery Today* **1997**, *2* (3), 102–109.
- Fitch, W. L.; Detre, G.; Holmes, C. P.; Shoolery, J. N.; Keifer, P. A. High-Resolution ¹H NMR in Solid-Phase Organic Synthesis. *J. Org. Chem.* **1994**, *59*, 7955–7956.
- Keifer, P. A.; Baltusis, L.; Rice, D. M.; Tymiak, A. A.; Shoolery, J. N. A Comparison of NMR Spectra Obtained for Solid-Phase-Synthesis Resins Using Conventional High-Resolution, Magic-Angle-Spinning, and High-Resolution Magic-Angle-Spinning Probes. *J. Magn. Reson. A* **1996**, *119*, 65–75.
- Keifer, P. A. Influence of Resin Structure, Tether Length, and Solvent upon the High-Resolution ¹H NMR Spectra of Solid-Phase-Synthesis Resins. *J. Org. Chem.* **1996**, *61*, 1558–1559.
- Sarkar, S. K.; Garigipati, R. S.; Adams, J. L.; Keifer, P. A. An NMR Method To Identify Nondestructively Chemical Compounds Bound to a Single Solid-Phase-Synthesis Bead for Combinatorial Chemistry Applications. *J. Am. Chem. Soc.* **1996**, *118*, 2305–2306.
- Garigipati, R. S.; Adams, B.; Adams, J. L.; Sarkar, S. K. Use of Spin-Echo Magic Angle Spinning ¹H NMR in Reaction Monitoring in Combinatorial Organic Synthesis. *J. Org. Chem.* **1996**, *61*, 2911–2914.
- Keifer, P. A. High-resolution NMR techniques for solid-phase synthesis and combinatorial chemistry. *Drug Discovery Today* **1997**, *2*, 468–478.
- Keifer, P. A. NMR Tools for Biotechnology. *Curr. Opin. Biotechnol.* **1999**, *10* (1), 34–41.
- Keifer, P. A. New methods for obtaining high-resolution NMR spectra of solid-phase synthesis resins, natural products, and solution-state combinatorial chemistry libraries. *Drugs Future* **1998**, *23*, 301–317.
- Smallcombe, S. H.; Patt, S. L.; Keifer, P. A. WET Solvent Suppression and its Applications to LC NMR and High-Resolution NMR Spectroscopy. *J. Magn. Reson. A* **1995**, *117*, 295–303.
- Smallcombe, S. H.; Patt, S. L.; Keifer, P. A. Solvent Suppression Method for LC-NMR and High-Resolution NMR. US Patent 5,847,564, 1998.
- Keifer, P. A. New NMR tools for combinatorial chemistry including solid-phase-synthesis-resin NMR and high-throughput spectroscopy. In *Book of Abstracts*; 213th ACS National Meeting, San Francisco, April 13–17 1997, ORGN-277; American Chemical Society: Washington, DC, 1997; pp ORGN-277.
- Sukumar, S.; Johnson, M. O. N.; Hurd, R. E.; Van Zijl, P. C. M. Automated Shimming for Deuterated Solvents Using Field Profiling. *J. Magn. Reson.* **1997**, *125*, 159–162.
- Rosen, M. E. Selective Detection in NMR by Time-Domain Digital Filtering. *J. Magn. Reson. A* **1994**, *107*, 119–125.
- Gilson, Inc., 3000 W. Beltline Hwy, P.O. Box 620027, Middleton, WI 53562, USA, 1-(800)-445-7661.
- Varian NMR Systems, Palo Alto, CA, USA; www.varianinc.com.
- Sun Microsystems, Inc., 901 San Antonio Rd., Palo Alto, CA 94303, USA.
- Varian NMR Systems, VNMR 6.1B Software, including VAST software package.
- National Scientific, 975 Progress Circle, Lawrenceville, GA 30043, (770)-995-7622, Part No. C4013-4045.
- Keifer, P. A. Flow Injection Analysis NMR (FIA-NMR)—A Novel Flow NMR Technique that Complements LC-NMR and Direct Injection NMR (DI-NMR). *Magn. Reson. Chem.* **2000**, in press.
- Ruzicka, J.; Hansen, E. H. *Flow Injection Analyses*; John Wiley and Sons: New York, 1988; pp 1–493.
- Karlberg, B.; Pacey, G. E. *Flow Injection Analysis – A Practical Guide*; Elsevier: New York, 1989; pp 1–367.
- Patt, S. L. Single- and Multiple-Frequency-Shifted Laminar Pulses. *J. Magn. Reson.* **1992**, *96*, 94–102.
- Smallcombe, S. H. Solvent Suppression with Symmetrically-Shifted Pulses. *J. Am. Chem. Soc.* **1993**, *115*, 4776–4785.
- Edzes, H. T. The Nuclear Magnetization as the Origin of Transient Changes in the Magnetic Field in Pulsed NMR Experiments. *J. Magn. Reson.* **1990**, *86*, 293–303.
- Philip F. Hughes, Sphinx Pharmaceuticals, Research Triangle Park, NC 27709, USA, unpublished results.
- Gorlach, E.; Richmond, R.; Lewis, I. High-Throughput Flow Injection Analysis Mass Spectrometry with Networked Delivery of Color-Rendered Results. 2. Three-Dimensional Spectral Mapping of 96-Well Combinatorial Chemistry Racks. *Anal. Chem.* **1998**, *70*, 3227–3234.
- Timothy D. Spitzer, Glaxo-Wellcome, Research Triangle Park, NC, unpublished results.
- ACD/Labs, 133 Richmond St. West, Suite 605, Toronto, Ontario, M5H 2L3, Canada; www.acdlabs.com.
- Kotyk, J. J.; Hoffman, N. G.; Hutton, W. C.; Bretthorst, G. L.; Ackerman, J. J. H. Comparison of Fourier and Bayesian analysis of NMR signals. II. Examination of truncated free induction decay NMR data. *J. Magn. Reson.* **1995**, *116*, 1–9.
- Bretthorst, G. L. Bayesian analysis. III. Applications to NMR signal detection, model selection, and parameter estimation. *J. Magn. Reson.* **1990**, *88*, 571–595.
- Simova, S.; Sengstschmid, H.; Freeman, R. Proton Chemical-Shift Spectra. *J. Magn. Reson.* **1997**, *124*, 104–121.
- Hu, H.; Van, Q. N.; Mandelshtam, V. A.; Shaka, A. J. Reference Deconvolution, Phase Correction, and Line Listing of NMR Spectra by the 1D Filter Diagonalization Methodol. *J. Magn. Reson.* **1998**, *134*, 76–87.
- Mandelshtam, V. A.; Van, Q. N.; Shaka, A. J. Obtaining Proton Chemical Shifts and Multiplets from Several 1D NMR Signals. *J. Am. Chem. Soc.* **1998**, *120*, 12161–12162.
- Mandelshtam, V. A.; Taylor, H. S.; Shaka, A. J. Application of the filter diagonalization method to one- and two-dimensional NMR spectra. *J. Magn. Reson.* **1998**, *133*, 304–312.
- Hajduk, P. J.; Olejniczak, E. T.; Fesik, S. W. One-Dimensional Relaxation- and Diffusion-Edited NMR Methods for Screening Compounds that Bind to Macromolecules. *J. Am. Chem. Soc.* **1997**, *119*, 12257–12261.
- Lin, M.; Shapiro, M. J.; Wareing, J. R. Diffusion-Edited NMR—Affinity NMR for Direct Observation of Molecular Interactions. *J. Am. Chem. Soc.* **1997**, *119*, 5249–5250.
- Wolfender, J.-L.; Rodriguez, S.; Hostettmann, K. Liquid chromatography coupled to mass spectrometry and nuclear magnetic resonance spectroscopy for the screening of plant constituents. *J. Chromatogr.* **1998**, *794*, 299–316.
- Morris, K. F.; Johnson, C. S., Jr. Resolution of discrete and continuous molecular size distributions by means of diffusion-ordered 2D NMR spectroscopy. *J. Am. Chem. Soc.* **1993**, *115*, 4291–4299.
- Barjat, H.; Morris, G. A.; Smart, S.; Swanson, A. G.; Williams, S. C. R. High-resolution diffusion-ordered 2D spectroscopy (HR-DOSY) – A new tool for the analysis of complex mixtures. *J. Magn. Reson. B.* **1995**, *108*, 170–172.
- Gonnella, N.; Lin, M.; Shapiro, M. J.; Wareing, J. R.; Zhang, X. Isotope-Filtered Affinity NMR. *J. Magn. Reson.* **1998**, *131*, 336–338.
- Lin, M.; Shapiro, M. J. Mixture Analysis in Combinatorial Chemistry. Application of Diffusion-Resolved NMR Spectroscopy. *J. Org. Chem.* **1996**, *61*, 7617–7619.
- Shuker, S. B.; Hajduk, P. J.; Meadows, R. P.; Fesik, S. W. Discovering High-Affinity Ligands for Proteins: SAR by NMR. *Science* **1996**, *274*, 1531–1534.

- (49) Tufte, E. R. *The Visual Display of Quantitative Information*; Graphics Press: Cheshire, CT, 1983; pp 1–197.
- (50) Gmeiner, W. H.; Cui, W.; Konerding, D. E.; Keifer, P. A.; Sharma, S. K.; Soto, A. M.; Marky, L. A.; Lown, J. W. Shape-Selective Recognition of a Model Okazaki Fragment by Geometrically-Constrained Bis-Distamycins. *J. Biomol. Struct. Dynam.* **1999**, *17*, in press.
- (51) Hamper, B. C.; Synderman, D. M.; Owen, T. J.; Scates, A. M.; Owsley, D. C.; Kesselring, A. S.; Chott, R. C. High-Throughput ¹H NMR and HPLC Characterization of a 96-Member Substituted Methylene Malonamic Acid Library. *J. Comb. Chem.* **1999**, *1*, 140–150.

CC990066U